



**THE PENNSYLVANIA
STATE UNIVERSITY**

(NASA-CR-142304) TELEOPERATOR CONTROL FOR
PASSIVATION OF SATELLITES POSSESSING ANGULAR
MOMENTUM (Pennsylvania State Univ.) 63 p HC
\$4.25 CSCL 22A

N75-18282

Unclas
12478

G3/15

**TELEOPERATOR CONTROL FOR PASSIVATION OF SATELLITES
POSSESSING ANGULAR MOMENTUM**

BY

ARUN A. NADKARNI

**ASTRONAUTICS RESEARCH REPORT
NO.75-2**

APRIL 1975

**DEPARTMENT OF AEROSPACE ENGINEERING
UNIVERSITY PARK, PENNSYLVANIA**



**RESEARCH PARTIALLY SUPPORTED BY NASA GRANTS NSG-7078
AND NGR 39-009-162**

ACKNOWLEDGMENTS

The author wishes to express his deep sense of gratitude to Dr. Marshall H. Kaplan, Associate Professor of Aerospace Engineering, for his valuable guidance and suggestions during the course of this work.

The work reported here was partially supported by NASA Grants NGR 39-009-162 and NSG-7078.

TABLE OF CONTENTS

	Page
ACKNOWLEDGMENTS.	ii
LIST OF TABLES	iv
LIST OF FIGURES.	v
NOMENCLATURE	vii
ABSTRACT	ix
I. INTRODUCTION	1
II. SATELLITE DYNAMICS	6
2.1 Approach-Rendezvous Phase	6
2.2 Satellite Motion Characteristics for the Capture Phase	8
III. SYSTEM EQUATIONS OF MOTION	13
3.1 Analysis of the Satellite Motion.	15
3.2 Analysis of Motion of the Combined Teleoperator- Satellite System.	17
3.3 Misalignment Between the Angular Momentum Vectors . .	23
3.4 Initial Conditions.	23
IV. RESULTS.	28
4.1 Motion of a Symmetric Satellite Under the Influence of External Passivating Torques	28
4.2 Motion of the Combined Teleoperator-Satellite System in an External Torque-Free Environment	37
V. CONCLUSIONS.	48
REFERENCES	49
APPENDIX: Teleoperator Design Modifications	50

LIST OF TABLES

Table		Page
I	Weight and Inertia Properties of Research Applications Module (RAM) Satellite	29
II	Initial Euler Rates of RAM Satellite.	29

LIST OF FIGURES

Figure		Page
1	Description of Combined Three-Axes Motion	3
2	Angular Velocity and Momentum Components for a Spinning and Precessing Satellite	3
3	Satellite Axes System	9
4	Coordinate Axes Frame for the Combined Teleoperator- Satellite System	14
5	Forms of Passivating Torque Functions Applied on the Three-Generalized Axes.	18
6	Coordinate Axes Frame for the Motion of Combined Teleoperator-Satellite System	25
7a	Misalignment of Angular Momentum Vectors.	26
7b	Initial Alignment of Combined System with Respect to Resultant Vector H_r	26
8	Motion of Satellite under the Influence of Passivating Torques, $K_1 = 1$, $K_2 = 1$, $K_3 = 2$	31
9	Motion of Satellite under the Influence of Passivating Torques, $K_1 = 1$, $K_2 = 1$, $K_3 = 3$	31
10	Motion of Satellite under the Influence of Passivating Torques, $K_1 = 1$, $K_2 = 1$, $K_3 = 4$	32
11	Motion of Satellite under the Influence of Passivating Torques, $K_1 = 1$, $K_2 = 2$, $K_3 = 1$	32
12	Motion of Satellite under the Influence of Passivating Torques, $K_1 = 2$, $K_2 = 1$, $K_3 = 1$	33
13	Motion of Satellite under the Influence of Passivating Torques, $K_1 = 2$, $K_2 = 1$, $K_3 = 2$	33
14	Motion of Satellite under the Influence of Passivating Torques, $K_1 = 2$, $K_2 = 1$, $K_3 = 5$	35
15	Motion of Satellite under the Influence of Passivating Torques, Zero Final State	35
16	Motion of Satellite under the Influence of Passivating Torques, $K_1 = 2$, $K_2 = 4$, $K_3 = 2$	36

LIST OF FIGURES (continued)

Figure		Page
17	Motion of Satellite under the Influence of Passivating Torques, $K_1 = 2$, $K_2 = 5$, $K_3 = 1$	36
18	Motion of Satellite under the Influence of Passivating Torques, $K_1 = 4$, $K_2 = 1$, $K_3 = 2$	38
19	Motion of Satellite under the Influence of Passivating Torques, $K_1 = 4$, $K_2 = 2$, $K_3 = 1$	38
20	Motion of the Asymmetric Teleoperator	39
21	Motion of Symmetric Teleoperator After Satellite Capture, Case 1	40
22	Motion of Symmetric Teleoperator After Satellite Capture, Case 2	42
23	Motion of Symmetric Teleoperator After Satellite Capture, Case 3	43
24	Motion of Symmetric Teleoperator After Satellite Capture, Case 4	44
25	Motion of Symmetric Teleoperator After Satellite Capture, Case 5	45
26	Motion of Symmetric Teleoperator After Satellite Capture, Case 6	47
27	Weight and Inertia Properties of Satellite Despin Model and Teleoperator.	51
28	Modified Design of Teleoperator	54

NOMENCLATURE

\vec{H}	Angular Momentum Vector
\vec{H}_r	Angular Momentum Vector of Combined Teleoperator-Satellite System
\vec{H}_s	Angular Momentum Vector of Satellite
\vec{H}_{To}	Angular Momentum Vector of Teleoperator
H_1	Component of \vec{H} Along x-Axis
H_2	Component of \vec{H} Along y-Axis
H_{12}	Component of \vec{H} in xy Plane
H_3	Component of \vec{H} Along z-Axis
$I_{x_s}, I_{y_s}, I_{z_s}$	Moments of Inertia of Satellite About Body Axes ox, oy, oz
$I_{x_r}, I_{y_r}, I_{z_r}$	Moments of Inertia of Teleoperator-Satellite System About Body Axes ox, oy, oz
K1, K2, K3	Constants Indicating Forms of Passivating Torques Applied
L	Lagrangian of the System
q_r	Generalized Coordinate System Relative to Orbit Plane
T	Kinetic Energy of the System
U	Potential Energy of the System
X, Y, Z	Moving Coordinate System Relative to Orbit Plane
x, y, z	Body-Fixed Coordinate System
θ, ϕ, ψ	Eulerian Angles Describing Motion of the Body
$\dot{\theta}, \dot{\phi}, \dot{\psi}$	Time Rate of Change of Euler Angles
τ_1, τ_2, τ_3	Passivating Torques in Generalized Directions
$\vec{\omega}$	Angular Velocity Vector
$\omega_x, \omega_y, \omega_z$	Components of Angular Velocity Vector Along Body Fixed Axes

NOMENCLATURE (continued)

Subscripts

cm	About Center of Mass
r, To/S	Resultant or Combined Teleoperator-Satellite System
S	Satellite
To	Teleoperator
1	Euler Variables of Combined Body
2	Euler Variables of Teleoperator Arm, Spindle, and Hand (Figure 4)

ABSTRACT

Certain space shuttle missions may require the retrieval of passive spinning and precessing satellites. One proposed means of retrieval utilizes a free-flying teleoperator launched from the shuttle. The feasibility of nulling the combined spin and precession (passivation) of a typical rigid satellite is first established using a Lagrangian formulation. It is shown that a proposed asymmetric teleoperator cannot be used for passivation in its present form because it would quickly tumble over after being spun-up to synchronize with the angular rates of the satellite. In addition, a dynamic analysis is made of the combined teleoperator-satellite system where an initial misalignment of their respective angular momentum vectors is assumed.

Chapter I

INTRODUCTION

With the development of the space shuttle system, space tug, and remote manipulator units (RMU's), it will soon be possible to maneuver satellites and other masses in orbit. Typically, such maneuvers are needed for the assembly of space stations, deployment of payloads, and retrieval of satellites for repair, refurbishment or removal. A satellite that is to be retrieved might well have some initial rotational angular momentum. Hence, for this satellite to be retrieved successfully, it may be imperative to be able to null its angular rates. This process is referred to as "passivation." A number of shuttle-based missions have already been identified which may require the retrieval of satellite payloads. These payloads include:

- i) Stabilized, normally-operating satellites which require periodic servicing or refurbishment. Stabilization of these satellites could be accomplished passively by spin-stabilization, or actively by reaction jets, control moment gyros (CMG's), or inertia wheels.

- ii) Freely-tumbling and/or spinning satellites. The Micrometeorite Exposure Module (MEM), for example, is currently conceived of as a non-stabilized passive satellite. Close inspection, removal and retrieval by the shuttle may be a requirement.

- iii) Satellites that have developed an attitude control system (ACS) malfunction. The nature of the malfunction may cause the satellite to be in a partially or completely unstabilized condition.

Typical satellites to be launched in the late 1970's and early 1980's for which retrieval might be required are listed in the study

conducted by Bell Aerospace Company.^(1,2) Criteria used in selecting satellites for study and their characteristics are tabulated in that study. The Research Application Module (RAM) is the most demanding⁽¹⁾ in terms of size and inertia for retrieval missions. This payload is of maximum possible size for the payload bay, and thus, imposes high accuracy requirements on shuttle positioning and stabilization of the teleoperator. The current configuration of the RAM indicates that it is to be CMG stabilized. However, gyro failure could cause motion about one or more axes during retrieval.

Dynamic state of a satellite being retrieved can range from a completely stabilized one to the worst case of combined three-axis tumbling. A satellite is said to be spinning when its angular momentum vector is along its longitudinal axis, and is said to be tumbling when this vector is along an arbitrary axis. Figure 1 shows a satellite coning about its angular momentum vector. The coning angle is influenced by the inertia properties of the satellite. Angular velocity can be expressed at any instant of time as the resultant of a spin component along the longitudinal axis and another component along the angular momentum vector \vec{H} , as shown in Figure 2. The angular momentum vector also could be expressed as a resultant vector of two corresponding components. If one of these components is zero, the satellite is in either a state of symmetric spin or flat spin. Utilizing an RMU to null these types of spin is straightforward. The RMU approaches the satellite along the axis of angular motion (i.e. along the angular momentum vector), then docks and applies torques to remove the angular momentum. The problem, however, is far more complicated for the general case when the satellite has both spin and tumble components of the angular velocity.

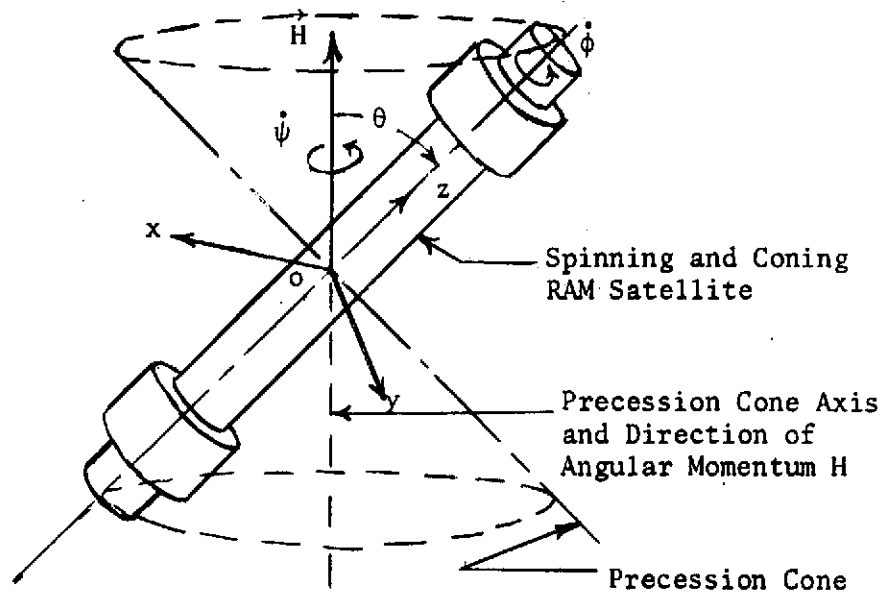


Figure 1. Description of Combined Three-Axes Motion.

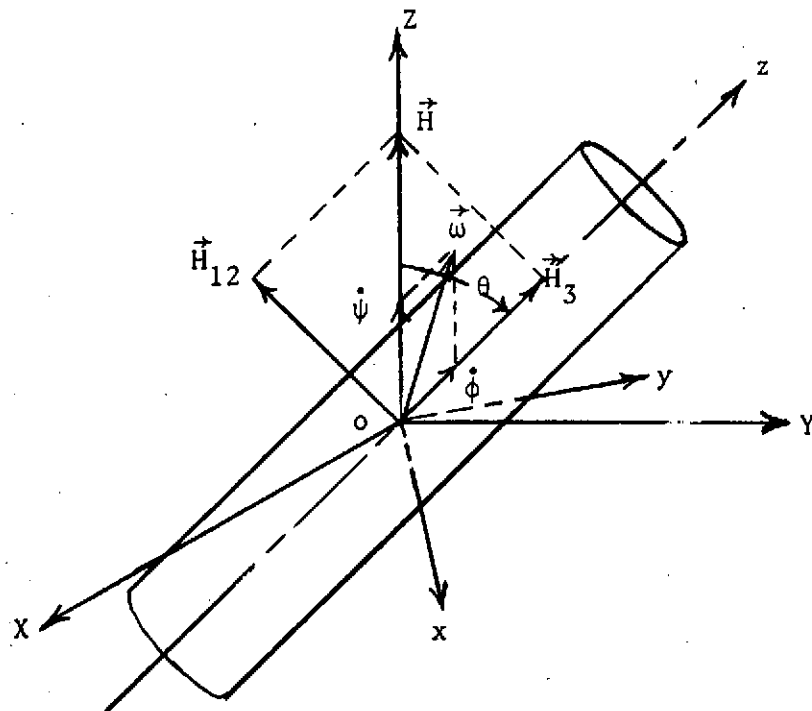


Figure 2. Angular Velocity and Momentum Components for a Spinning and Precessing Satellite.

In this case, it is not only necessary to synchronize the teleoperator with the spinning and nutation rates of the satellite, but to adjust the grappling arm to the nutation cone angle.

A limited amount of study has already been done to analyze "free-flying" and "shuttle-attached" teleoperators for retrieval purposes. This work has determined broad performance requirements needed by the teleoperators in order to retrieve typical satellites from orbit. Based on this, a baseline "free-flying" teleoperator concept was established and a preliminary plan developed for its implementation.^(1,2) Specific objectives included determination of teleoperator performance requirements for typical satellite configurations and for typical dynamic conditions expected during the encounter. A study conducted by Faile et al.⁽³⁾ considered a more complicated case of dynamic passivation of a spinning and precessing object, by applying various torques to the satellites. In most of these studies, it is assumed that the momentum vector of the teleoperator coincides with that of the satellite. This is, however, an oversimplification of the situation encountered during an actual maneuver. Firstly, it is difficult to synchronize the nutation and spin rates of the teleoperator arms with those of the satellite. Secondly, it is difficult to align the teleoperator exactly along the satellite momentum vector for final rendezvous. Finally, it is difficult to determine the exact alignment of the satellite momentum vector itself. Thus, it would be desirable to study the resultant motion of the combined teleoperator-satellite system for a certain degree of misalignment between the two momentum vectors. This has been achieved here by allowing the angular rates and the nutation angle of the teleoperator arms to differ slightly from the predetermined, fixed

values for the rates and the angle of the satellite. The misalignment between the two momentum vectors is then calculated and the combined body analyzed for its resulting motion.

The feasibility of nulling the combined spin and precession of a typical rigid satellite is first established using a Lagrangian formulation. Next it is shown that a proposed asymmetric teleoperator cannot be used in its present configuration for passivation because it would quickly tumble over after being spun-up to synchronize with the angular rates of the satellite. Finally, a dynamic analysis is made of the combined teleoperator-satellite system where an initial misalignment of their respective angular momentum vectors is assumed.

Chapter II

SYSTEM DYNAMICS

The system and function requirements for each mission are discussed in detail in Ref. 2. System requirements include those of performance, information, interface, and support. The overall function requirements e.g., approach-rendezvous phase, capture phase, and recovery phase may be accomplished by either a free-flying or attached-boom teleoperator. Although the numerous tasks required for a free-flying teleoperator (FFTO) during the three phases may differ slightly in detail from those for an attached-boom teleoperator, they apply equally for both the cases.

2.1 Approach-Rendezvous Phase

It is assumed that the teleoperator is carried in the shuttle payload bay during launch. A deployment mechanism is needed to provide a fly-off/dock station, which is positioned well away from the bay to assure safe operations. This mechanism could be a telescopic boom or a truss-type structure. When the FFTO reaches the vicinity of the satellite, one or two circumnavigations may be necessary in order to inspect the satellite and determine its angular momentum vector. This information is essential for aligning the FFTO in the appropriate approach direction for docking.

As indicated previously, the RAM satellite was found to be the most demanding with respect to the function requirements. Expected yaw, ω_x pitch, ω_y and roll, ω_z rates for various failure modes of the RAM satellite as indicated in Ref. 2 are listed below:

i) An abnormal shut-down of the satellite's attitude control system (ACS) followed by an extended period of satellite drift would develop:

$$\omega_x = \omega_y \leq 0.025 \text{ rad/sec.}$$

$$\omega_z \leq 0.1 \text{ rad/sec.}$$

(ii) A failure of the ACS about one axis:

(a) failure in roll would develop:

$$\omega_x, \omega_y \leq 0.1 \text{ rad/sec.}$$

$$\omega_z \leq 10 \text{ rad/sec.}$$

(b) failure in pitch or yaw would develop:

$$\omega_x, \omega_y \leq 1 \text{ rad/sec.}$$

$$\omega_z \leq 1 \text{ rad/sec.}$$

(iii) A failure of the satellite ACS about more than one axis would develop:

$$\omega_x, \omega_y \leq 1 \text{ rad/sec.}$$

$$\omega_z \leq 10 \text{ rad/sec.}$$

The nutation cone angle θ depends upon the ratio of the combined pitch-yaw rate (ω_{xy}) to the roll rate (ω_z). This coning angle is zero for a pure spin ($\omega_{xy} = 0$). When the coning angle is small, the preferred approach for capture with convenience may be along the momentum vector to the end face of the satellite (end approach). However, when this angle is large, the preferred approach may be to the waist of the satellite at the center of mass (waist approach). The rendezvous phase ends with the FFTO about 20 to 50 feet away from the satellite along the final approach direction, as established by the inspection maneuver.

2.2 Satellite Motion Characteristics for the Capture Phase

Consider a cylindrical, symmetric satellite as shown in Figure 3, which is both spinning and tumbling in space. When these angular rates are passive, i.e., there are no external torques acting on the satellite initially, the total angular momentum vector \vec{H} of the satellite is fixed in direction in inertial space. The body continues to spin about its longitudinal axis and to precess or cone about the angular momentum vector at a constant coning angle θ . In the absence of any external torques, the coning angle θ and the spin and precession rates remain constant for a symmetrical satellite.

Before one can successfully take the satellite to the shuttle, it is imperative to null its angular rates. This can only be done by eliminating the angular momentum of the satellite, i.e., nulling the individual components of the angular momentum vector. This is possible by applying torques to the body through teleoperator gripping arms in directions opposite to those of the $\vec{\omega}$ components. There are obviously many ways of applying torques to the body, depending upon the design and geometry of teleoperator arms (see Appendix for one such design). For a teleoperator with a freely spinning spindle at the end of the "hand", a passivating torque may be applied along the pitch or yaw axis of the satellite, which is easier than to try to reduce its spin rate. This observation is especially true if the teleoperator hand is designed to lock onto a docking ball located at the center of the satellite end face. Here it is obvious that the magnitude of the despinning torque applied by the teleoperator along the roll axis of the satellite is limited, as the docking ball is situated on or very near the spin-axis of the satellite. If the teleoperator is designed to approach the

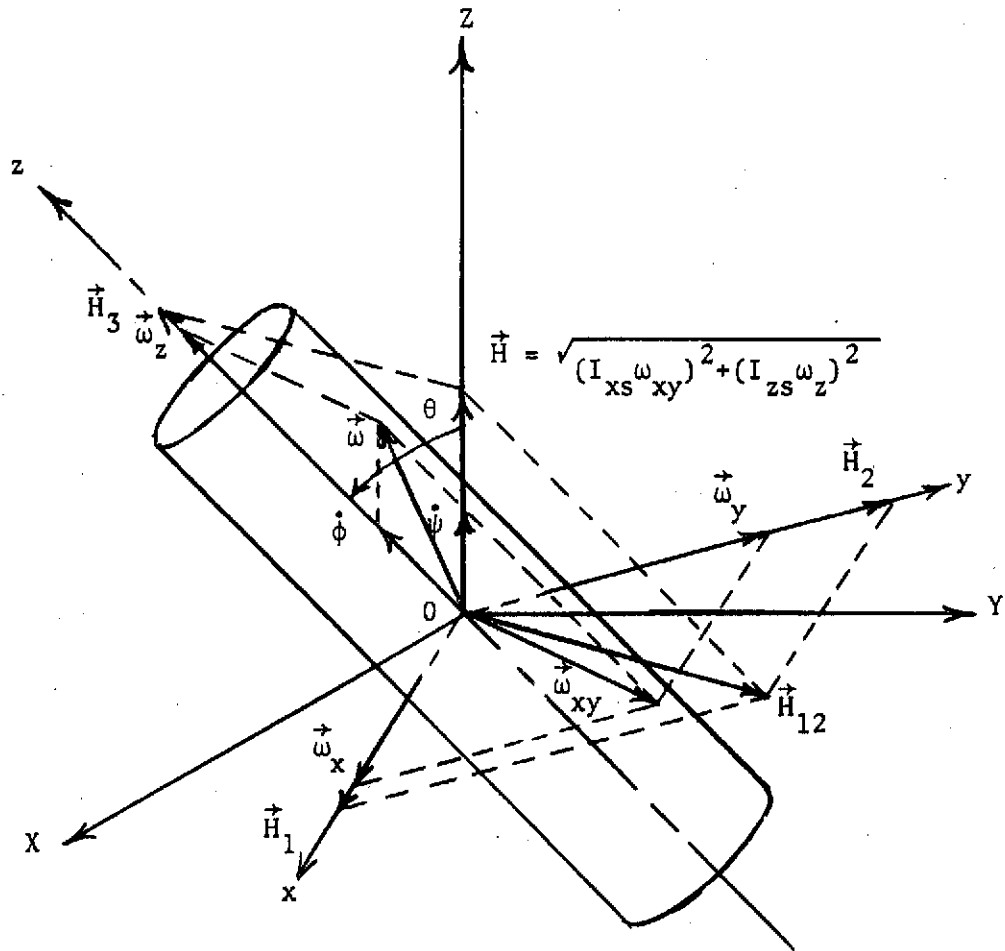


Figure 3. Satellite Axes System.

ORIGINAL PAGE IS
OF POOR QUALITY

spinning satellite from one end by tracking the center of the satellite as in the end approach, the magnitude of applied pitch or yaw torque would be much more than that of the rolling or despinning torque it can apply. The teleoperator is in a position to despin the satellite very effectively, if it is designed with a grappling jaw mounted on a spindle synchronized with the spin rate of the satellite, and the jaw grips the satellite at the waist. Thus, the ways to nullify components of momentum may be broadly classified into three approaches:

- 1) eliminate either the spin component or the precession component and then the other,
- 2) eliminate both components simultaneously by applying torques on spin and precession axes, or
- 3) eliminate both components simultaneously by applying torques on spin and precession axes and a torque to simultaneously reduce the coning angle. This last procedure is found to passivate the satellite at the fastest rate.

Suppose it is desired to eliminate the precession component of \vec{H} first. It would then be necessary to apply a torque opposite in direction to that of the precession component. Application of this torque will obviously cause some drift of the total momentum vector, depending on the magnitude of the passivating torque applied. Thus, a torque of small magnitude will have to be applied over a long period of time to limit drift of the momentum vector within reasonable bounds. At the end of this period the precession component of \vec{H} would be completely removed, and the total angular momentum is then in simple spin. In actual practice, however, the angle θ will not be reduced exactly to zero during this process. There will be some residual

up its arms and hand to synchronize exactly with the precession and spin rate of the satellite. The hand orientation is simultaneously adjusted to match the coning angle. The teleoperator is now in a position to capture the satellite smoothly, without introducing impact forces and torques. However, in practical rendezvous situations it is difficult to achieve this exact alignment of the two angular momentum vectors. Hence, it is also difficult to achieve perfect synchronization of the rates of the two vehicles. Thus, in practice, the teleoperator approaches the satellite along a direction slightly different from the direction of its momentum vector. It then tries to capture the satellite with its arms and hand which are spinning at slightly different rates than those of the satellite. It is essential to study the motion of the combined body after capture to ensure that the teleoperator does not tumble over or go into an unstable mode.

The analysis of a system of rigid bodies, rotating at different angular rates and connected rigidly, is presented in detail by Martz⁽⁴⁾ and Greenwood.⁽⁵⁾ The solution of the second order, non-linear equations of motion describing the motion in terms of Eulerian angles, expressed in elliptic functions, is given by Whittaker.⁽⁶⁾ However, we derive the equations of motion of the composite body by Lagrangian formulation and solve them on a digital computer by using second order Runge-Kutta method of integration.

After capturing the satellite in its arms, the teleoperator returns to the shuttle. This phase is known as the recovery phase. No complicated maneuvers between the two masses are anticipated.

Chapter III

SYSTEM EQUATIONS OF MOTION

The complete equations of motion, describing the motion of the rigid satellite under the influence of despinning and detumbling torques and the motion of the combined teleoperator-satellite after the capture phase, are derived in this chapter. These equations describe the motion of the two systems in terms of Eulerian angles. Coordinate systems used, along with the various dynamical parameters, such as the components of the angular momentum vector \vec{H} , the angular velocity vector $\vec{\omega}$, etc., are shown in Figures 3 and 4.

Figure 3 shows the coordinate system used for the satellite moving under the influence of passivating torques. The XYZ coordinate system is the moving coordinate frame in the orbit, with X-axis directed outwards along the radius vector; Y-axis being perpendicular to the orbit plane and the Z-axis lying in the orbit plane to complete the right handed system. The xyz system is the body fixed coordinate system rotating with the satellite. The z-axis is the longitudinal axis of the satellite along the axis of symmetry in the present case. The x-axis and the y-axis are any two axes, located perpendicular to the z-axis and passing through an origin at the center of mass. Their exact location is immaterial because of symmetry. The location of the body axes referenced to the moving frame is described with the help of three Euler angles. The corresponding coordinate frames for the combined teleoperator-satellite system is shown in Figure 4. In this case, the origin of the XYZ-moving frame is located at the center of mass of the

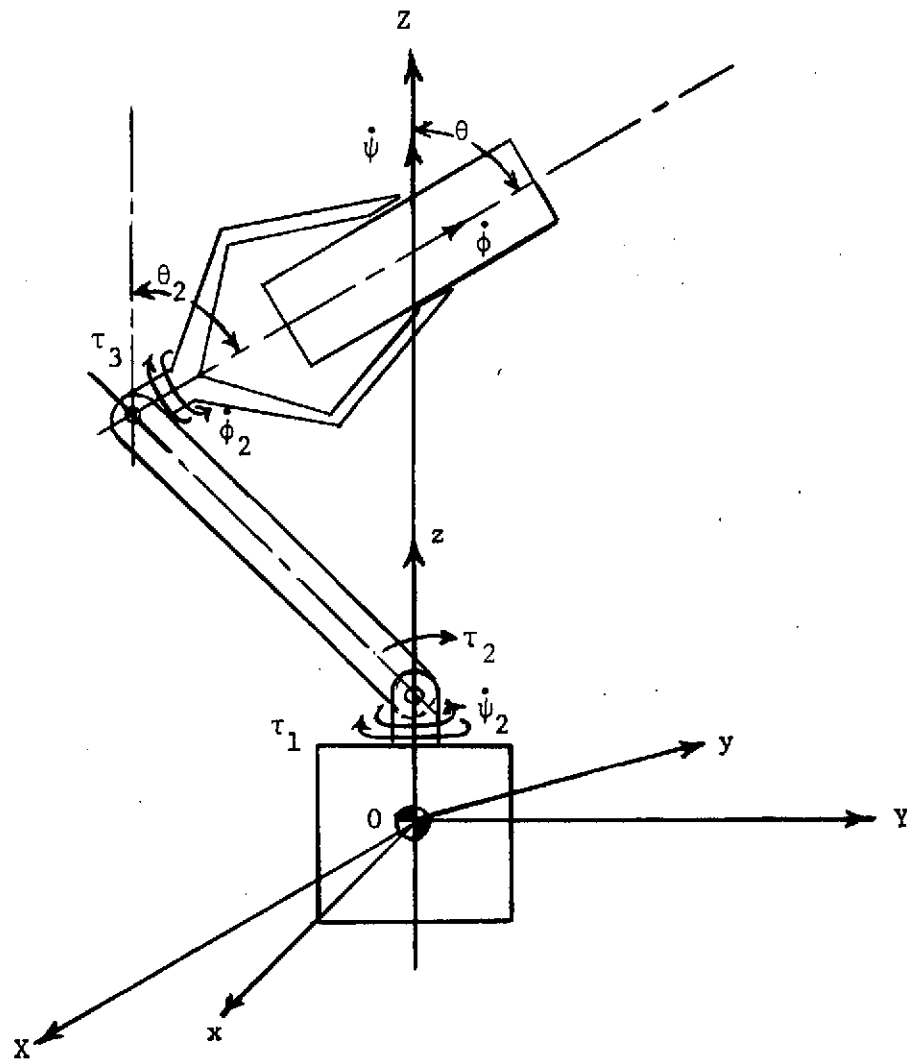


Figure 4. Coordinate Axes Frame for the Combined Teleoperator-Satellite System.

control unit of the teleoperator. The xyz-system is again the body-fixed system, with the x-axis (and hence the y-axis) being arbitrarily chosen initially. The location of the body axes is once again described relative to the moving XYZ-frame with the help of three Euler angles.

3.1 Analysis of the Satellite Motion

Non-constant angular velocities under the influence of the despinning and detumbling torques. The equations of motion of the satellite, moving under the influence of the applied torques, can be derived from the total kinetic energy T_s of the satellite via a Lagrangian formulation. The total kinetic energy T_s of a symmetric tumbling body is

$$T_s = \frac{1}{2} [I_{x_s} \omega_x^2 + I_{y_s} \omega_y^2 + I_{z_x} \omega_z^2] \quad (1)$$

From the geometry of the Figure 3, it is seen that

$$\omega_z = \dot{\phi} + \dot{\psi} \cos \theta \quad (2)$$

$$\omega_{xy}^2 = \omega_x^2 + \omega_y^2 = \dot{\psi}^2 \sin^2 \theta + \dot{\theta}^2 \quad (3)$$

and

$$I_{x_s} = I_{y_s} \quad (4)$$

$$\therefore T_s = \frac{1}{2} I_{x_s} [\dot{\psi} \sin \theta]^2 + \frac{1}{2} I_{x_s} \dot{\theta}^2 + \frac{1}{2} I_{z_s} [\dot{\phi} + \dot{\psi} \cos \theta]^2 \quad (5)$$

Now, the Euler-Lagrange equations of motion for a rigid body are

(Ref. 5)

$$\frac{d}{dt} \left(\frac{\partial L}{\partial \dot{q}_r} \right) - \frac{\partial L}{\partial q_r} = \tau_r \quad (6)$$

where Lagrangian $L = T - U$, and τ_r = generalized force in the direction of the r^{th} generalized coordinate.

In the present case, since we are interested in only relative motion of the satellite with respect to the moving frame, we neglect the potential energy U of the satellite. In view of this, differentiating the expression for the kinetic energy of the satellite with respect to the three generalized coordinates, i.e., the three Eulerian angles, will yield the equations of motion of the satellite, as follows:

ψ direction:

$$\begin{aligned} & (I_{x_s} \sin^2 \theta + I_{z_s} \cos^2 \theta) \ddot{\psi} + 2 (I_{x_s} - I_{z_s}) \sin \theta \cos \theta \dot{\theta} \dot{\psi} \\ & + I_{z_s} (\ddot{\phi} \cos \theta - \dot{\theta} \sin \theta \dot{\theta}) = \tau_1 \end{aligned} \quad (7)$$

θ direction:

$$I_{x_s} \ddot{\theta} + (I_{z_s} - I_{x_s}) \dot{\psi}^2 \sin \theta \cos \theta + I_{z_s} \dot{\phi} \dot{\psi} \sin \theta = \tau_2 \quad (8)$$

ϕ direction:

$$I_{z_s} (\ddot{\phi} + \ddot{\psi} \cos \theta - \dot{\psi} \dot{\theta} \sin \theta) = \tau_3 \quad (9)$$

These particular directions (along the Euler angles ψ , θ , and ϕ) are chosen, because the design of the teleoperator is such that it will be applying passivating torques to the satellite in these directions.

These equations can be solved exactly with the help of elliptic functions if $\tau = 0$. However, in the present analysis, these second-order, coupled, differential equations were solved on the digital computer using second-order Runge-Kutta method of integration. Various despinning and/or detumbling torque functions were tried in each of the generalized directions. The torque functions used were:

a) zero torque; b) a torque of constant magnitude; c) a torque proportional to the angular rate or the coning angle; d) a combination of the cases (b) and (c); and e) a triangular torque function.

The forms of all these torque functions are shown in Figures 5a through 5d.

3.2 Analysis of Motion of the Combined Teleoperator-Satellite System

Under torque-free conditions. In the last section we analyzed the motion of the symmetric satellite, moving under the influence of the external despinning and detumbling torques applied through the gripping arms of the teleoperator. These passivating torques could be applied only after the satellite is firmly held in the arms of the teleoperator. In most of the previous analyses, it was tacitly assumed that the angular momentum vector of the teleoperator coincides exactly with that of the satellite. Under these conditions, the passivation of the satellite would be a fairly easy task for a symmetric teleoperator-satellite combination. However, in practical rendezvous situations, it will be most improbable that the teleoperator will approach the satellite exactly along its angular momentum vector. In addition, since the angular rates of the arms and hand of the teleoperator are to be synchronized with the precession and spin rates of the satellite only after a short observation pass, there is bound to be some difference in the rates and the coning angle of the two bodies. Due to the uncertainties involved, it seems appropriate to allow for some deviation in the alignment of the angular momentum vector of the teleoperator from that of the satellite. In the present analysis, this is achieved by

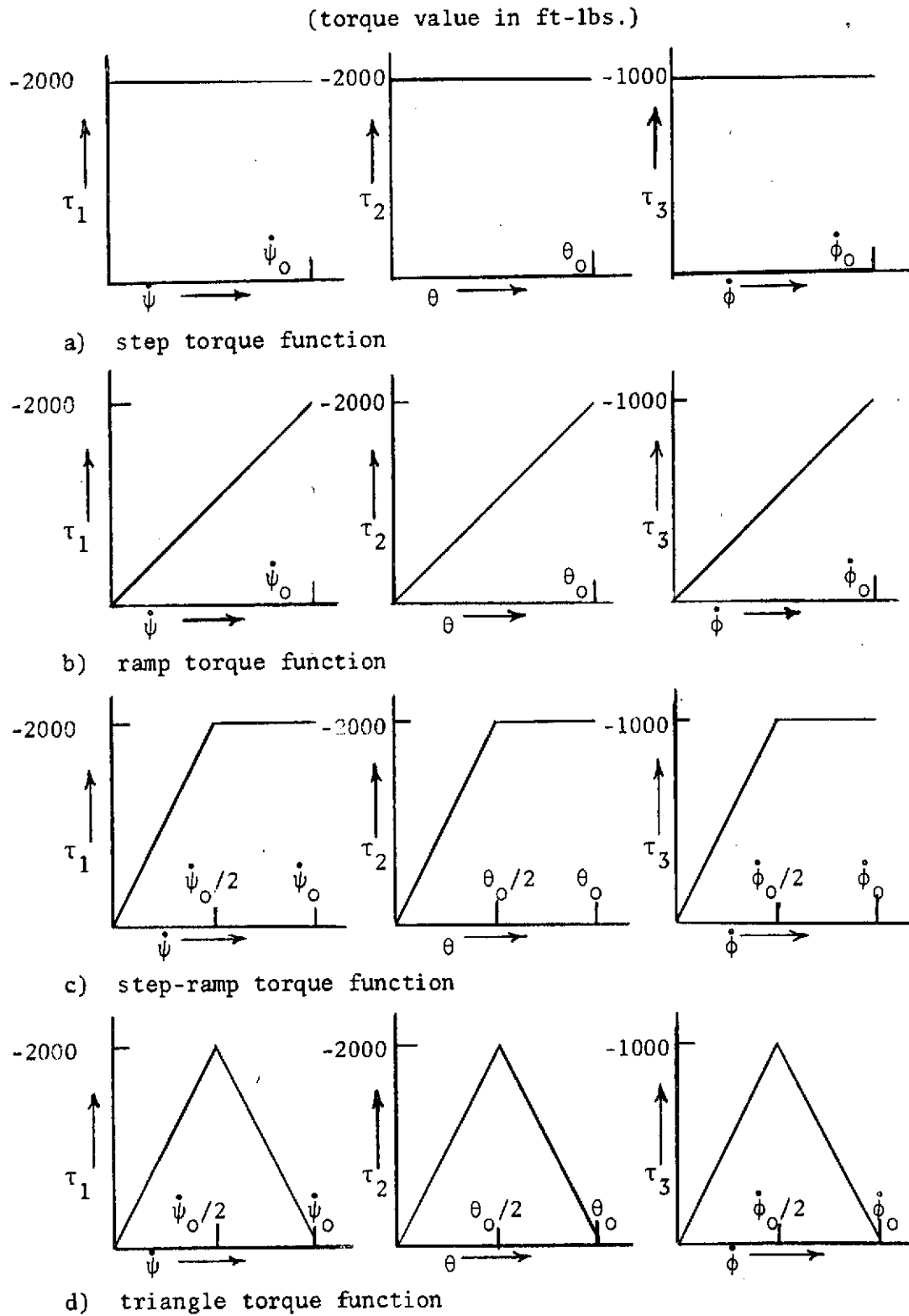


Figure 5. Forms of Passivating Torque Functions Applied on the Three-Generalized Axes.

either i) assuming different angular rates for the teleoperator from the prescribed precession rate and spin rate of the satellite, or ii) different hand angle for the teleoperator from the coning angle of the satellite. It is further assumed that the teleoperator mass is an order of magnitude greater than the mass of the satellite. Once the teleoperator arms grasp the satellite, the satellite starts moving with the angular rates prescribed by the arms and its angular momentum vector is recalculated.

With the help of the Lagrangian formulation, the equations of motion of the combined teleoperator-satellite mass are derived using the expression for the total kinetic energy of the system. This total energy is given by

$$T_{To/S} = \frac{1}{2} [I_{x_r} \omega_x^2 + I_{y_r} \omega_y^2 + I_{z_r} \omega_z^2] \quad (10)$$

Again, from the geometry of Figure 6,

$$\omega_x = \dot{\psi}_1 \sin \theta_1 \sin \phi_1 + \dot{\theta}_1 \cos \phi_1 \quad (11)$$

$$\omega_y = \dot{\psi}_1 \sin \theta_1 \cos \phi_1 - \dot{\theta}_1 \sin \phi_1 \quad (12)$$

$$\omega_z = \dot{\phi}_1 + \dot{\psi}_1 \cos \theta_1 \quad (13)$$

Substituting these values of ω_x , ω_y , and ω_z into the equation (10) yields

$$\begin{aligned} T_{To/S} = & \frac{1}{2} I_{x_r} (\dot{\psi}_1 \sin \theta_1 \sin \phi_1 + \dot{\theta}_1 \cos \phi_1)^2 \\ & + \frac{1}{2} I_{y_r} (\dot{\psi}_1 \sin \theta_1 \cos \phi_1 - \dot{\theta}_1 \sin \phi_1)^2 \\ & + \frac{1}{2} I_{z_r} (\dot{\phi}_1 + \dot{\psi}_1 \cos \theta_1)^2 \end{aligned} \quad (14)$$

Now, utilizing the Euler-Lagrange equations of motion for a rigid body⁽⁵⁾

$$\frac{d}{dt} \frac{\partial L}{\partial \dot{q}_r} - \frac{\partial L}{\partial q_r} = \tau_r \quad (15)$$

as before, and differentiating the expression for the kinetic energy of the composite mass with respect to the three generalized coordinates, viz., the three Eulerian angles ψ_1 , θ_1 , and ϕ_1 , will yield the equations of motion of the composite teleoperator-satellite mass, as follows:

ψ_1 direction:

$$\begin{aligned} & (I_{x_r} \sin^2 \theta_1 \sin^2 \phi_1 + I_{y_r} \sin^2 \theta_1 \cos^2 \phi_1 + I_{z_r} \cos^2 \theta_1) \ddot{\psi}_1 \\ & + [2I_{x_r} (\sin \theta_1 \cos \theta_1 \sin^2 \phi_1 \dot{\theta}_1 + \sin^2 \theta_1 \sin \phi_1 \cos \phi_1 \dot{\phi}_1) \\ & + 2I_{y_r} (\sin \theta_1 \cos \theta_1 \cos^2 \phi_1 \dot{\theta}_1 - \sin^2 \theta_1 \cos \phi_1 \sin \phi_1 \dot{\phi}_1) \\ & - 2I_{z_r} (\cos \theta_1 \sin \theta_1 \dot{\theta}_1)] \dot{\psi}_1 + I_{x_r} \{ \sin \theta_1 \sin \phi_1 \cos \phi_1 \ddot{\theta}_1 \\ & + \cos \theta_1 \sin \phi_1 \cos \phi_1 \dot{\phi}_1^2 + \dot{\theta}_1 \sin \theta_1 (\cos^2 \phi_1 - \sin^2 \phi_1) \dot{\phi}_1 \} \\ & - I_{y_r} \{ \sin \theta_1 \sin \phi_1 \cos \phi_1 \ddot{\theta}_1 + \cos \theta_1 \sin \phi_1 \cos \phi_1 \dot{\theta}_1^2 \end{aligned}$$

$$\begin{aligned}
& + \ddot{\theta}_1 \sin \theta_1 (\cos^2 \phi_1 - \sin^2 \phi_1) \dot{\phi}_1 \} + I_{z_r} \{ \ddot{\phi}_1 \cos \theta_1 - \dot{\phi}_1 \sin \theta_1 \dot{\theta}_1 \} \\
& = \tau_{\psi_1}
\end{aligned} \tag{16}$$

θ_1 direction:

$$\begin{aligned}
& (I_{x_r} \cos^2 \phi_1 + I_{y_r} \sin^2 \phi_1) \ddot{\theta}_1 + [I_{x_r} \dot{\psi}_1 \cos \theta_1 \sin \phi_1 \cos \phi_1 \\
& - 2I_{x_r} \cos \phi_1 \sin \phi_1 \dot{\phi}_1 - I_{y_r} \dot{\psi}_1 \cos \theta_1 \sin \phi_1 \cos \phi_1 \\
& + 2I_{y_r} \sin \phi_1 \cos \phi_1 \dot{\phi}_1] \dot{\theta}_1 + [I_{x_r} (\ddot{\psi}_1 \sin \theta_1 \sin \phi_1 \cos \phi_1 \\
& + \dot{\psi}_1 \sin \theta_1 \{ \cos^2 \phi_1 - \sin^2 \phi_1 \} \dot{\phi}_1) - I_{y_r} (\ddot{\psi}_1 \sin \theta_1 \sin \phi_1 \cos \phi_1 \\
& + \dot{\psi}_1 \sin \theta_1 \{ \cos^2 \phi_1 - \sin^2 \phi_1 \} \dot{\phi}_1)] - [I_{x_r} \dot{\psi}_1^2 \sin \theta_1 \cos \theta_1 \sin^2 \phi_1 \\
& + I_{x_r} \dot{\psi}_1 \dot{\theta}_1 \sin \phi_1 \cos \phi_1 \cos \theta_1 + I_{y_r} \dot{\psi}_1^2 \cos^2 \phi_1 \sin \theta_1 \cos \theta_1 \\
& - I_{y_r} \dot{\psi}_1 \dot{\theta}_1 \sin \phi_1 \cos \phi_1 \cos \theta_1 - I_{z_r} \dot{\psi}_1^2 \sin \theta_1 \cos \theta_1 \\
& - I_{z_r} \dot{\psi}_1 \dot{\theta}_1 \sin \theta_1] = \tau_{\theta_1}
\end{aligned} \tag{17}$$

ϕ_1 direction:

$$I_{z_r} \ddot{\phi}_1 + I_{z_r} (\ddot{\psi}_1 \cos \phi_1 - \dot{\psi}_1 \sin \theta_1 \dot{\theta}_1)$$

$$\begin{aligned}
& - [I_{x_r} (\dot{\psi}_1^2 \sin^2 \theta_1 \sin \phi_1 \cos \phi_1 - \dot{\theta}_1^2 \sin \phi_1 \cos \phi_1 \\
& + 2 \dot{\psi}_1 \dot{\theta}_1 \sin \theta_1 \{ \cos^2 \phi_1 - \sin^2 \phi_1 \}) \\
& + I_{y_r} (- \dot{\psi}_1^2 \sin^2 \theta_1 \sin \phi_1 \cos \phi_1 + \dot{\theta}_1^2 \sin \phi_1 \cos \phi_1 \\
& - 2 \dot{\psi}_1 \dot{\theta}_1 \sin \theta_1 \{ \cos^2 \phi_1 - \sin^2 \phi_1 \})] = \tau_{\phi_1} \quad (18)
\end{aligned}$$

Since we analyze the motion of the combined teleoperator-satellite system in an external torque-free environment, the torques τ_{ψ_1} , τ_{θ_1} , and τ_{ϕ_1} in the above expressions are identically equal to zero. Also, in view of the assumption that the angular rates of the teleoperator are imparted instantaneously to the satellite, we do not consider the relative motion between the two masses.

These non-linear, coupled, differential equations were again solved on a digital computer using the second order Runge-Kutta method of integration. It should be noted at this stage that a preliminary design of a single arm teleoperator, used by the Bell Aerospace Co.⁽²⁾ and shown in the Appendix, is very unstable, even without the spinning and precessing satellite in its hold. If its arm and the gripping hand are spun to the desired angular rates (at which the satellite is observed to be precessing and spinning), the teleoperator tumbles over completely in less than 2 secs as is shown in Chapter IV dealing with results. To correct this situation, a modification of the Bell design is proposed in this work. Accordingly, the Bell design is modified so that the teleoperator consists of four arms and hands, the hands are

synchronized to rotate at the same angular rates (although these rates may differ from the spin rate of the satellite). The hands rotate in such a way that the +z-components of their angular momentum add up and the x or y components cancel out each other. This design of the teleoperator, as shown in the Appendix, is found to be quite stable when its arms and hands are rotating at the prescribed angular rates. In all the following results then, only this modified design of the teleoperator is considered.

3.3 Misalignment Between the Angular Momentum Vectors

As was explained in the previous sections, this misalignment between the angular momentum vector of the teleoperator and that of the satellite is simulated here by considering the cases when one or all the three variables of the teleoperator differ from those for the satellite. The three variables for the teleoperator are: a) the angular velocity of the spindle (theoretically matching with the precession rate of the satellite); b) the angle that the hand makes with the +z-axis (matching with the coning angle); and c) the angular velocity of the hand (matching with the spin velocity of the satellite).

3.4 Initial Conditions

The misalignment angle is the angle which the +z-axis of the composite body (assumed to be coinciding with the +z-axis of the symmetric teleoperator) makes with the resultant angular momentum vector which remains stationary in space. To calculate this angle and the initial location of the body-fixed coordinate frame xyz of the composite

body (Fig. 6) with respect to the inertially oriented angular momentum vector \vec{H}_r of the composite body, we assume that after the satellite is gripped firmly in the arms of the teleoperator, it picks up the rotational rates imposed on it by the arms. This makes the angular momentum vector \vec{H}_s of the satellite drift from the original +z direction by an angle θ_3 , given by the following relationship.

$$\theta_3 = \tan^{-1} \frac{I_{xs_{cm}} \omega_{xy}}{I_{zs_{cm}} \omega_z} \quad (19)$$

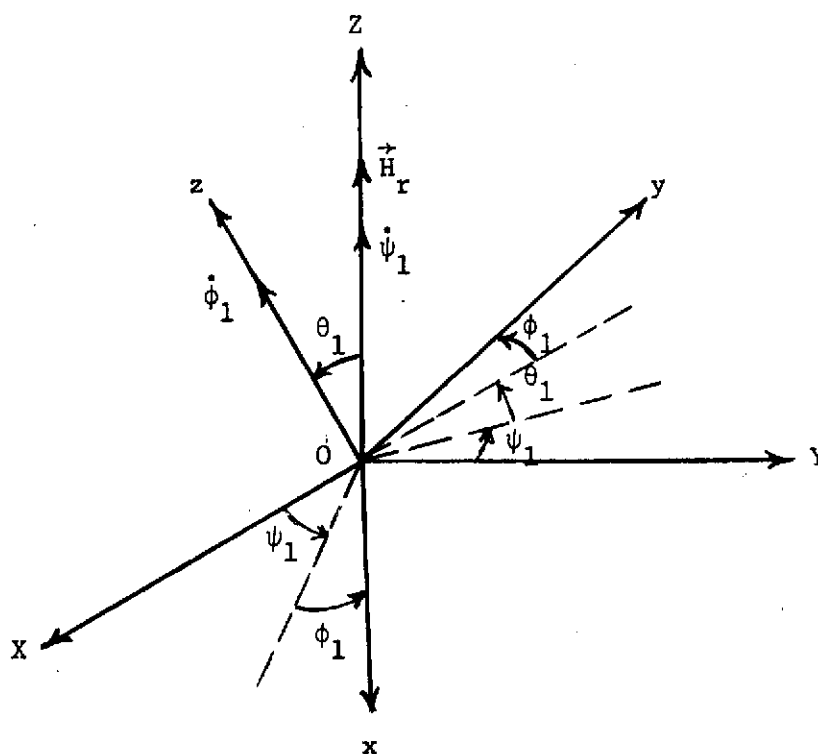
Let us assume that the hand of the teleoperator may have an initial misalignment, then if the actual angle it makes with the +z-axis in the satellite-fixed body frame is θ_2 , the net misalignment angle which the \vec{H}_s vector makes with the +z-axis in the teleoperator-fixed body frame is (Fig. 7a)

$$\theta_E = \theta_2 - \theta_3 \quad (20)$$

The resultant momentum vector \vec{H}_r of the composite body could then be easily calculated, and the angle θ_o which the vector \vec{H}_r makes with the +z-axis in the teleoperator-fixed body frame, is as shown in Figure 7a, given by

$$\theta_o = \sin^{-1} \frac{H_s \sin \theta_E}{H_r} \quad (21)$$

Now, if the x-axis of the teleoperator-fixed body frame coincides initially with the y-axis of the moving frame, the initial values of the Euler angles and angular rates are from Figure 7b as follows,



ORIGINAL PAGE IS
OF POOR QUALITY

Figure 6. Coordinate Axes Frame for the Motion of Combined Teleoperator-Satellite System.

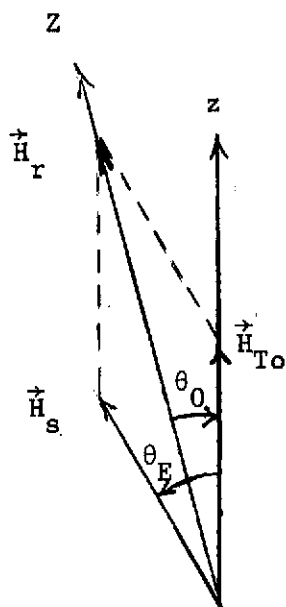


Figure 7a. Misalignment of Angular Momentum Vectors.

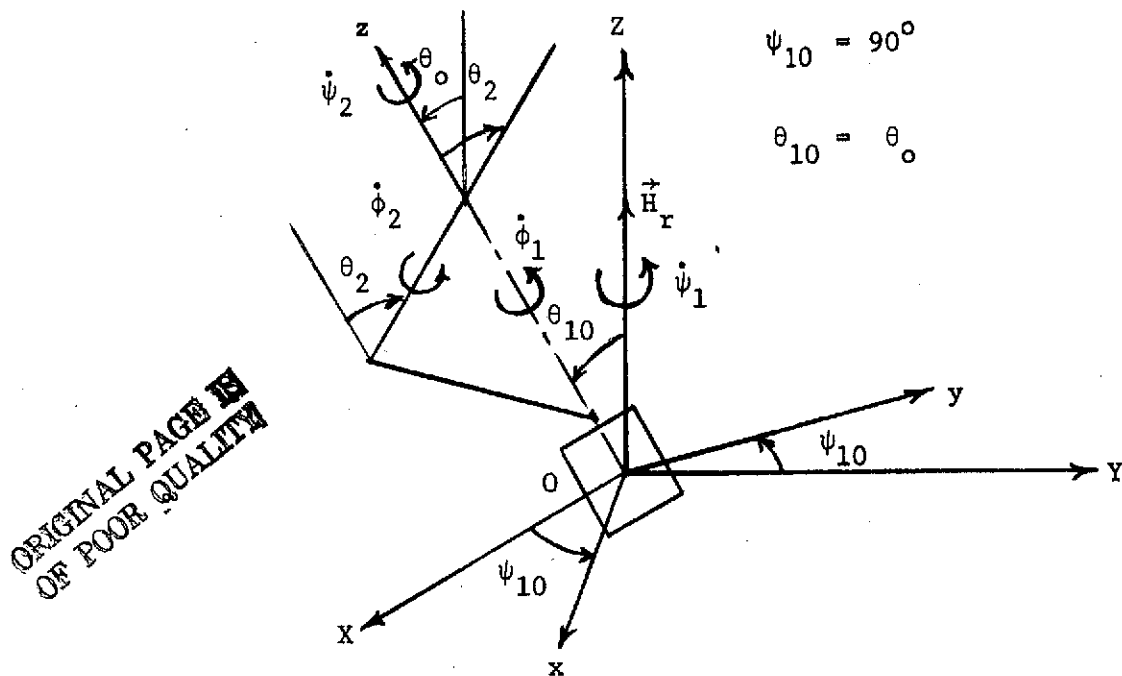


Figure 7b. Initial Alignment of Combined System with Respect to Resultant Vector H_r .

$$\psi_1 = \pi/2 \quad (22)$$

$$\dot{\psi}_1 = \dot{\psi}_2 \cos \theta_0 + \dot{\phi}_2 \cos \theta_2 \quad (23)$$

$$\theta_1 = \theta_0 \quad (24)$$

$$\dot{\theta}_1 = 0 \quad (25)$$

$$\phi_1 = 0 \quad (26)$$

$$\dot{\phi}_1 = \dot{\psi}_2 + \dot{\phi}_2 \cos (\theta_2 + \theta_0) \quad (27)$$

Now, we proceed to solve the second order, coupled, differential equations of motion from these initial conditions.

Chapter IV

RESULTS

The results presented in this chapter can be classified in two categories. In the first one, only the motion of the satellite under the action of the various torque functions is presented. In the second case, the motion of the combined teleoperator-satellite mass system is presented, both for the case when the angular momentum vector of the teleoperator coincides with that of the satellite and for the cases when it does not.

4.1 Motion of a Symmetric Satellite Under the Influence of External Passivating Torques

Figures 5a through 5d show the types of torque functions that were applied to the satellite. Although all possible combinations of these torque functions, applied in the ψ -direction, θ -direction, and the ϕ -direction were tested, only a few relevant results are presented in the Figures 8 through 19. To indicate the combination of torque functions applied on the three generalized directions, indicators K1, K2, and K3 are noted on each of the Figures 8 through 19. For instance, for the case when K1 = 1, K2 = 1, and K3 = 1, it indicates that no passivating torques were applied to the satellite; the motion is therefore torque-free motion. Similarly, when K1 = 2, K2 = 1, and K3 = 2, it indicates that constant torques of magnitudes shown in Figure 5a were applied to the satellite in the ψ and ϕ directions, whereas no torque was applied in the θ direction, and so on.

The inertia properties of the satellite are described in Table I and the initial Euler rates of its motion are tabulated in Table II.

Table I

Weight and Inertia Properties of
Research Applications Module (RAM) Satellite

Weight	= 20,000 lbs. = 9071.84 kg
Length	= 60 ft. = 18.29 m.
Diameter	= 11 ft. = 3.3528 m.
I_{xx}	= 157,000 lb. ft. ² = 6615.98 kg. m. ²
I_{yy}	= 157,000 lb. ft. ² = 6615.98 kg. m. ²
I_{zz}	= 7,050 lb. ft. ² = 297.09 kg. m. ²

Table II

Initial Euler Rates of the RAM Satellite

$\dot{\psi}$	= 0.46 rad/sec.
$\dot{\phi}$	= 4.0 rad/sec.
θ	= 65.9°

Figure 8 shows the motion of the satellite, when a constant torque is applied only in the ϕ -direction. The satellite spin rate is reduced to almost zero in 28 secs. and the satellite goes into a flat tumble with the coning angle of about 90° and precessing at the original rate. A satellite is said to be in a state of flat tumble, when it is spinning with its angular momentum vector along one of its transverse body axes.

Figure 9 shows the motion of the satellite, when a torque proportional to the spin rate is applied to the satellite on its spin axis. The rate of passivation of the satellite about the spin axis is slower, but the coning angle also increases at a slower rate than in the previous case. Thus, it is seen that the spin velocity of the satellite is reduced to a value below 0.5 rad/sec. in about 50 secs., whereas the coning angle increases asymptotically to a value of 90° .

Figure 10 shows the motion when a step-ramp torque is applied only about the spin axis. The rate of spin-passivation is faster than in the previous case, this being compensated by slightly higher coning angles.

Figure 11 shows the motion when a constant torque is applied only on the θ -axis. It is seen that the spin rate is not affected at all; the coning angle continues to oscillate, and the precession rate though slightly oscillatory in nature keeps increasing over a period of time.

Figure 12 indicates the motion when a constant torque is applied only about the ψ -axis of the satellite. The spin rate is observed to be unaffected, the satellite precession rate is passivated within permissible limits within 23 secs., but the satellite assumes a position at an angle of about 26° with $+z$ -axis. Figure 13 indicates the various angular rates of the satellite when a constant torque acts on both the precession and spin axes, with no torque applied on the θ -axis. The spin rate is passivated within 28 secs. and the precession rate within 29 secs. At the end of this period, the satellite assumes a position at about 81° with the $+z$ -axis. Figure 14 shows the motion

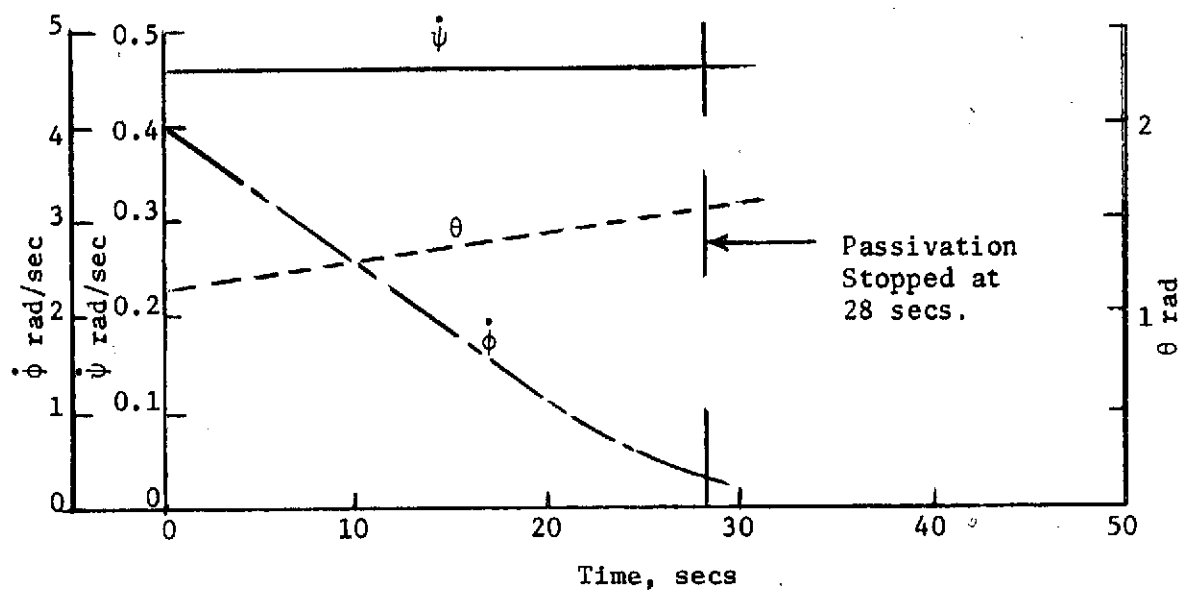


Figure 8. Motion of Satellite under the Influence of Passivating Torques, $K_1 = 1$, $K_2 = 1$, $K_3 = 2$.

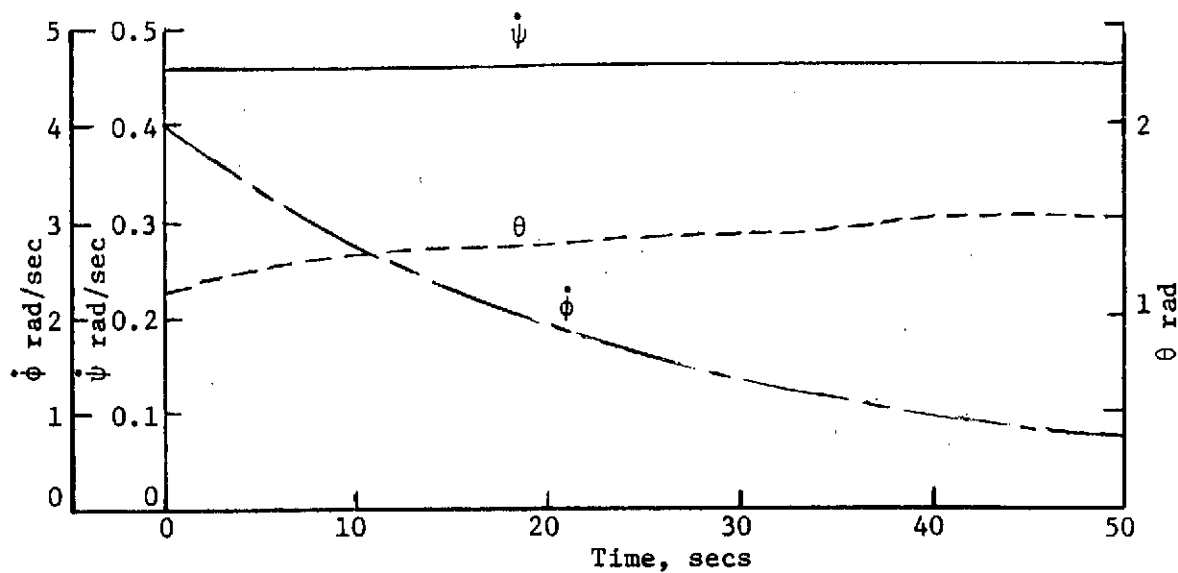


Figure 9. Motion of Satellite under the Influence of Passivating Torques, $K_1 = 1$, $K_2 = 1$, $K_3 = 3$.

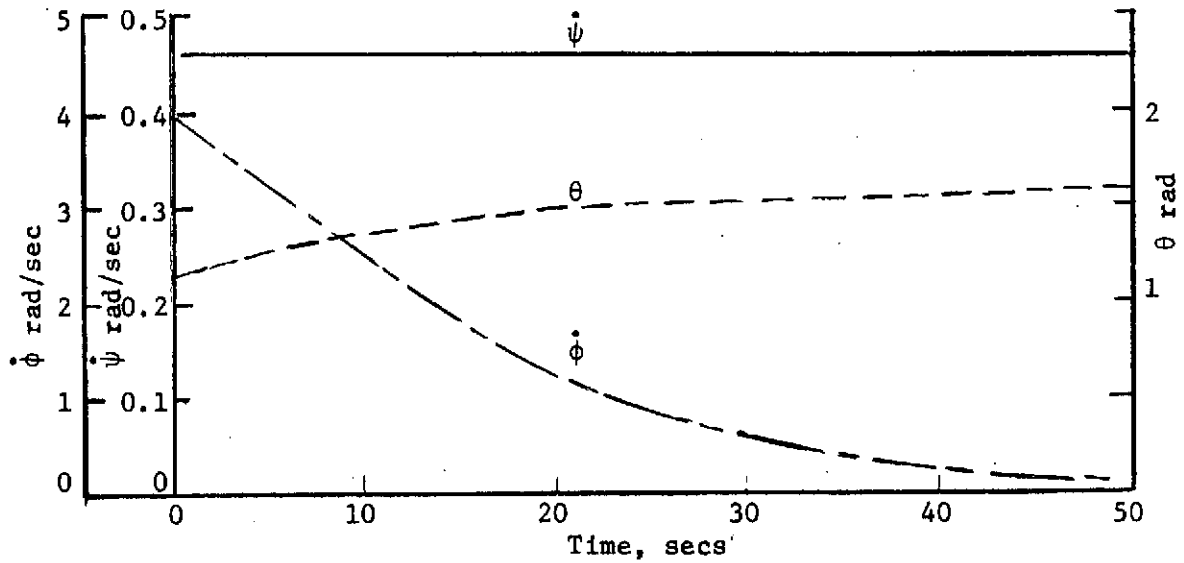


Figure 10. Motion of Satellite under the Influence of Passivating Torques, $K_1 = 1$, $K_2 = 1$, $K_3 = 4$.

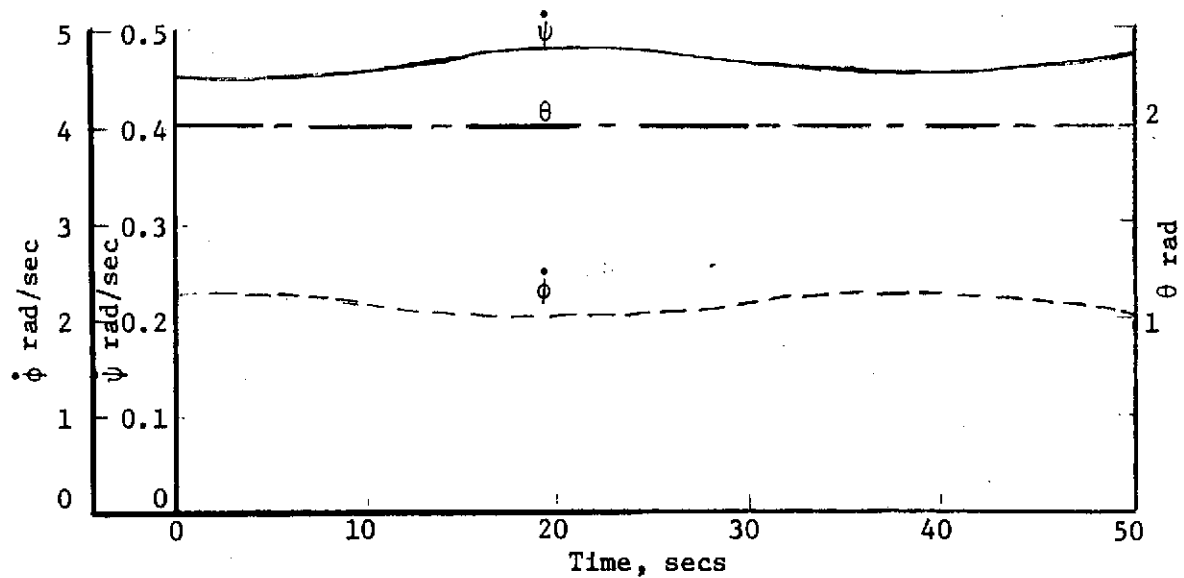


Figure 11. Motion of Satellite under the Influence of Passivating Torques, $K_1 = 1$, $K_2 = 2$, $K_3 = 1$.

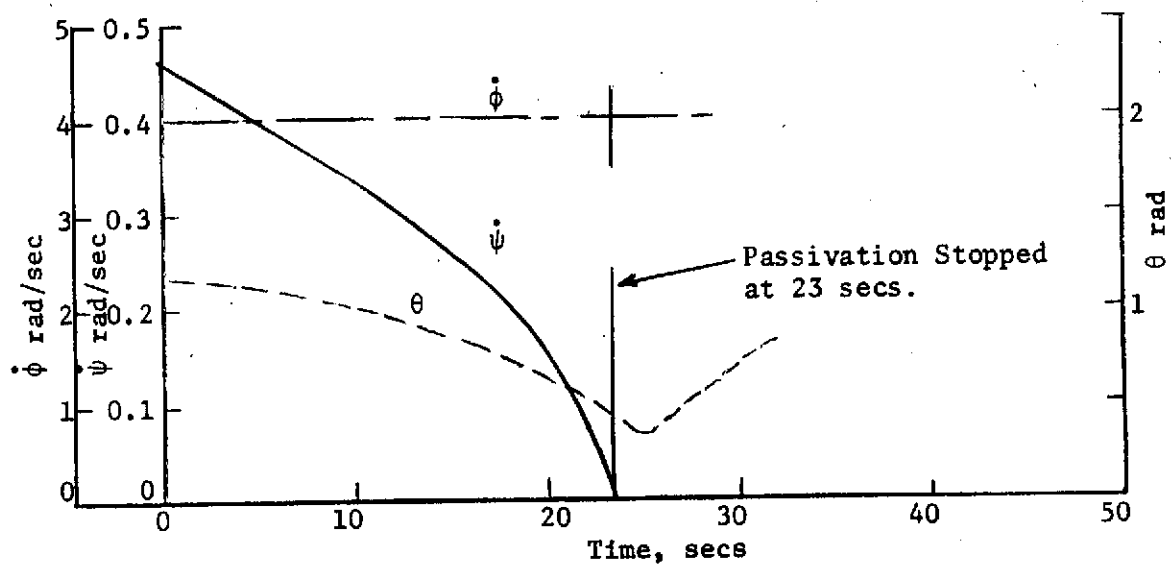


Figure 12. Motion of Satellite under the Influence of Passivating Torques, $K_1 = 2$, $K_2 = 1$, $K_3 = 1$.

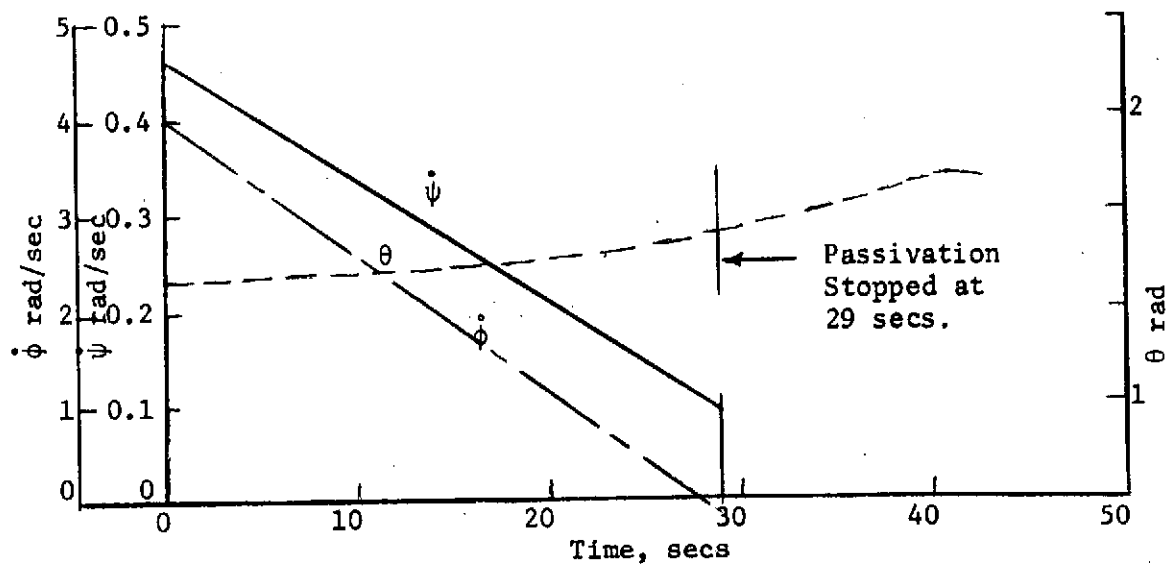


Figure 13. Motion of Satellite under the Influence of Passivating Torques, $K_1 = 2$, $K_2 = 1$, $K_3 = 2$.

when a constant torque is applied on the ψ -axis and a triangular torque function is forced on the spin or ϕ -axis. The precession is passivated within 24 secs. and the spin rate is also reduced. In addition, the coning angle is reduced to about 34° . Figure 15 shows the sequence of torque functions applied when it is desired to passivate all the three Eulerian variables, $\dot{\psi}$, θ , and $\dot{\phi}$. With the sequence shown, the spin is passivated within 28 secs., precession in an additional 6 secs., and the deconing is completed in another 4 secs. Thus, the satellite is completely passivated in 40 secs. It is seen from the figure that the decelerations imparted to the satellite are fairly regular. Thus, this mode of passivation may be best suited to retrieve disabled manned-space capsules. Also, the teleoperator arm geometry cannot allow the satellite to reach a pure tumble state. Hence, this may also be preferred sequence of passivation for highly spinning satellites. Figure 16 shows the motion when a constant torque is applied about the precession and spin axes and a step-ramp function on the θ -axis. The despinning is completed within 28 secs. and the precession and coning is reduced in a total of 40 secs., but by that time, a spin velocity of sufficient magnitude in opposite direction is imparted to the satellite. So, the passivation is stopped at 28 secs. Figure 17 shows the situation when a constant torque is applied on the precession axis, a triangular torque function on the θ -axis, and no torque on the spin axis. The spin rate is totally unaffected and the satellite detumbles and decones within 22 secs. The decelerations imparted to the satellite, however, are severe. Figure 18 shows the motion when a step-ramp torque function is applied on the precession

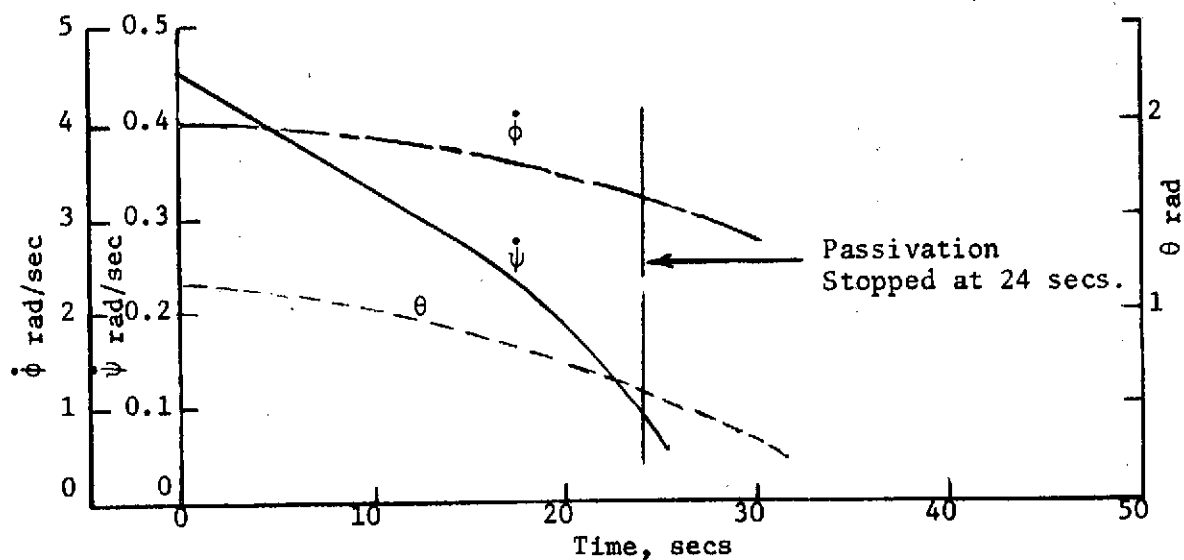


Figure 14. Motion of Satellite under the Influence of Passivating Torques, $K_1 = 2$, $K_2 = 1$, $K_3 = 5$.

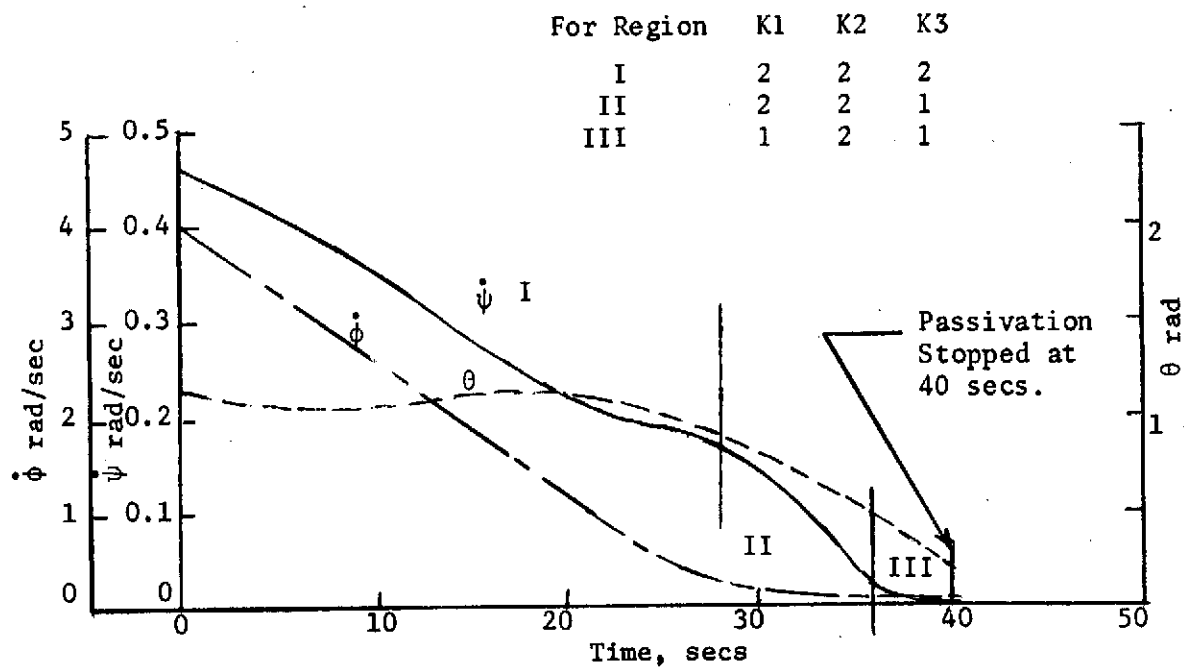


Figure 15. Motion of Satellite under the Influence of Passivating Torques, Zero Final State.

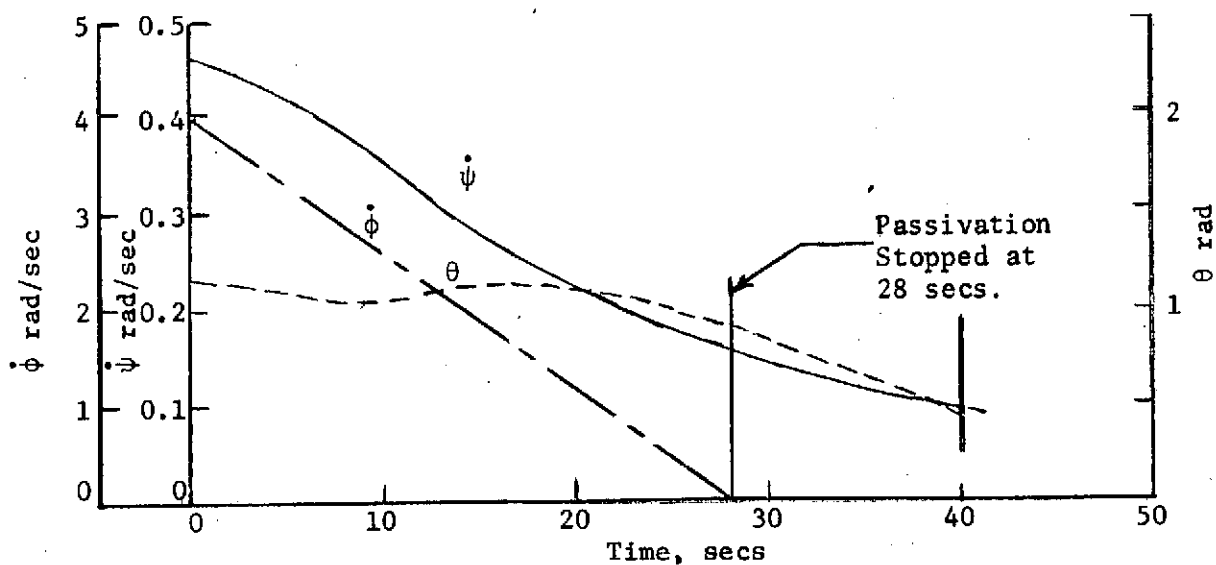


Figure 16. Motion of Satellite under the Influence of Passivating Torques, $K_1 = 2$, $K_2 = 4$, $K_3 = 2$.

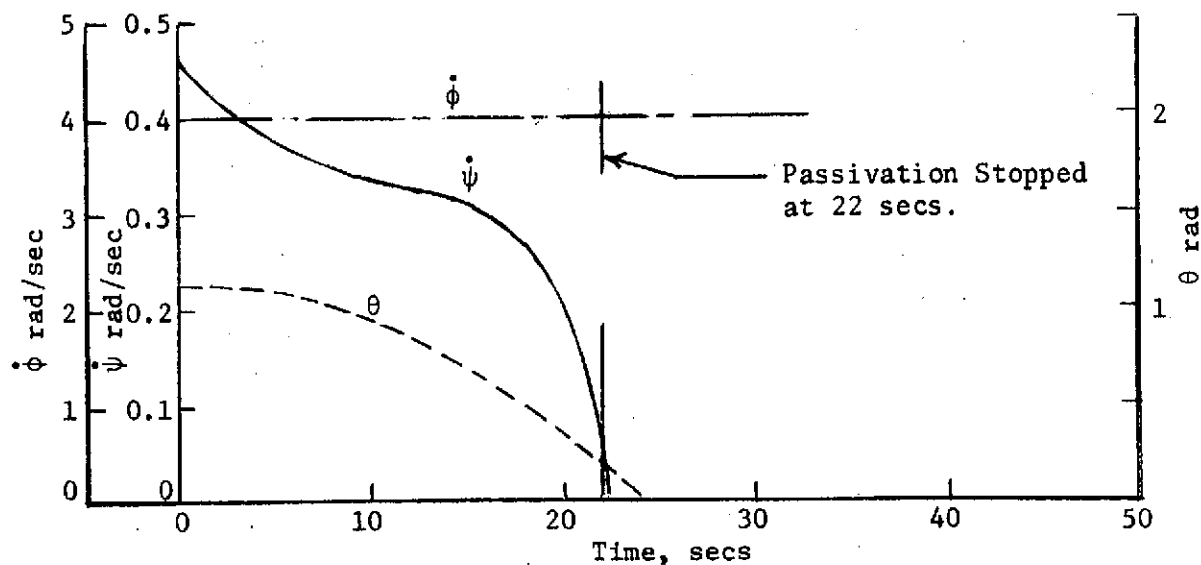


Figure 17. Motion of Satellite under the Influence of Passivating Torques, $K_1 = 2$, $K_2 = 5$, $K_3 = 1$.

axis, a constant torque on the spin axis, and no torque on the θ -axis. The spin is passivated within 28 secs., with the precession rate being considerably reduced. The cone angle, however, approaches 90° , thus this procedure may not be suitable when the arm geometry does not allow the holding of the satellite at 90° . Figure 19 shows the motion when a step-ramp torque is applied on the precession axis, a constant torque on the θ -axis, and the spin axis is left torque free. The spin of the satellite is not affected, and the precession and coning is nullified within 23 secs. This procedure may be useful for slowly spinning satellites which are precessing at high angular rates at fairly large coning angles.

4.2 Motion of the Combined Teleoperator-Satellite System in an External Torque-Free Environment

As was pointed out in earlier sections, the asymmetric teleoperator, as designed by the Bell Aerospace Co.⁽²⁾ was found to tumble over in less than 2 secs. Figure 20 shows the angular rates and the coning angle of the longitudinal $+z$ -axis. The mass and inertia properties of this teleoperator are listed in the Appendix. Since the teleoperator should be stable while approaching the satellite, only the improved, symmetric design as described in the Appendix is considered. Figure 21 shows the motion of the teleoperator-satellite combination. In this case, the angular velocity of the spindle coincides exactly with the precession rate of the satellite, the spin rate of the arm coincides with the spin rate of the satellite, and the angle of the arm, θ_2 , coincides with the coning angle, θ , of the satellite. It is seen that

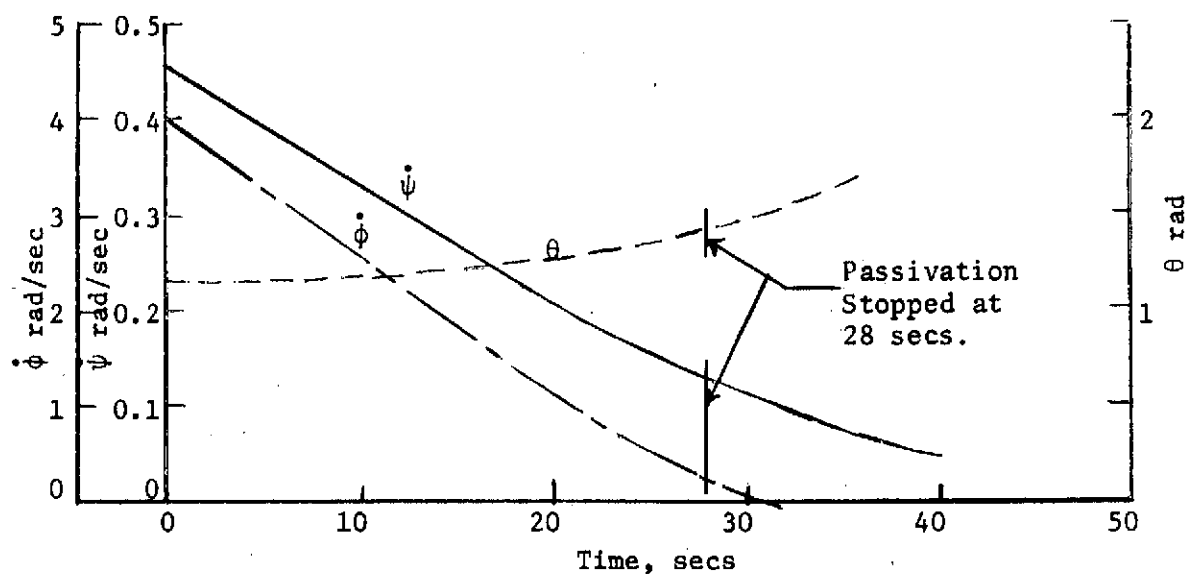


Figure 18. Motion of Satellite under the Influence of Passivating Torques, $K_1 = 4$, $K_2 = 1$, $K_3 = 2$.

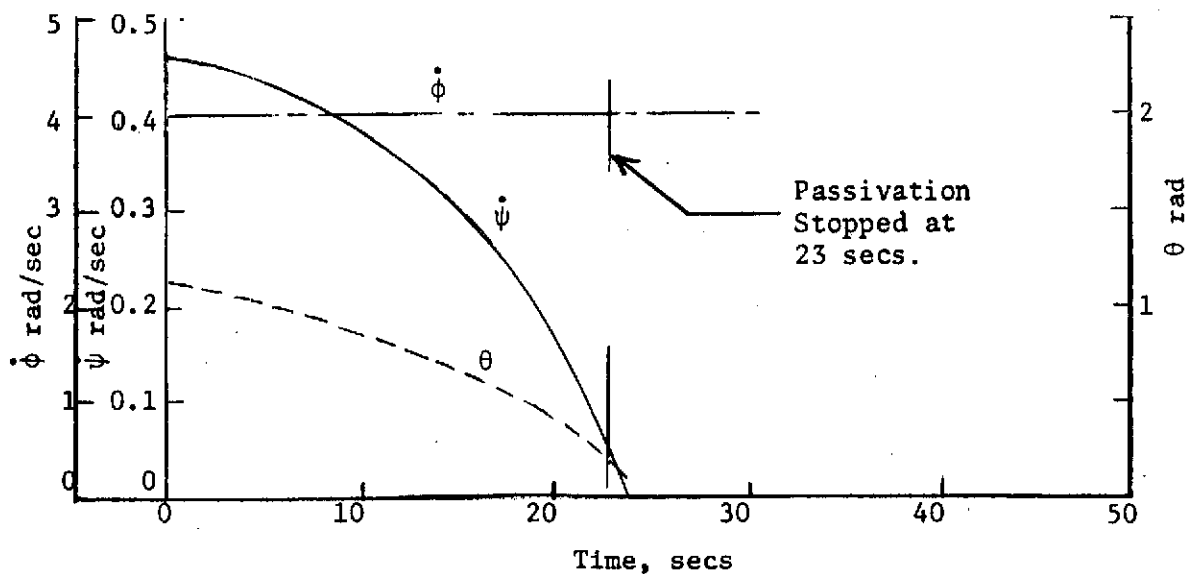


Figure 19. Motion of Satellite under the Influence of Passivating Torques, $K_1 = 4$, $K_2 = 2$, $K_3 = 1$.

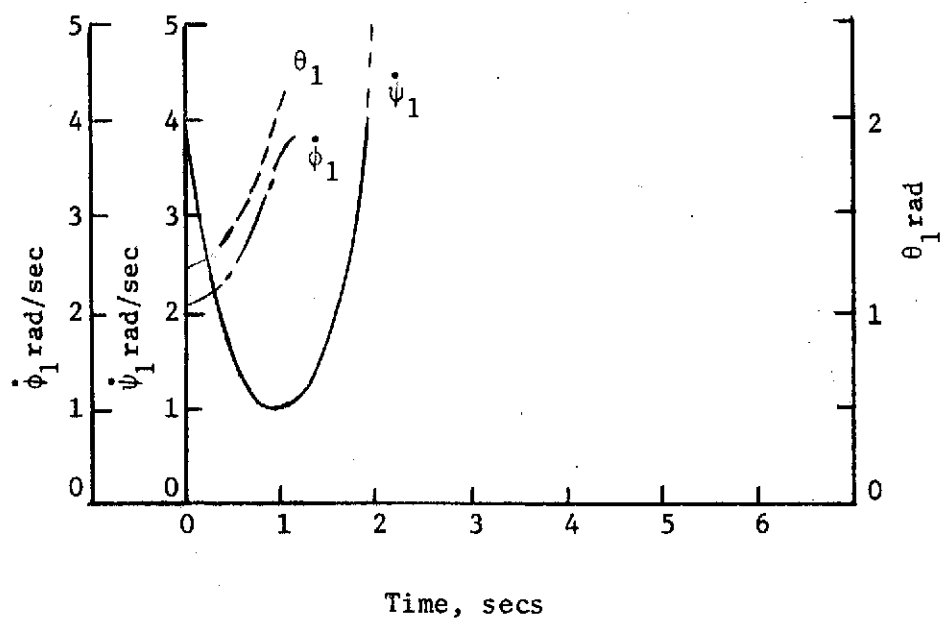


Figure 20. Motion of the Asymmetric Teleoperator.

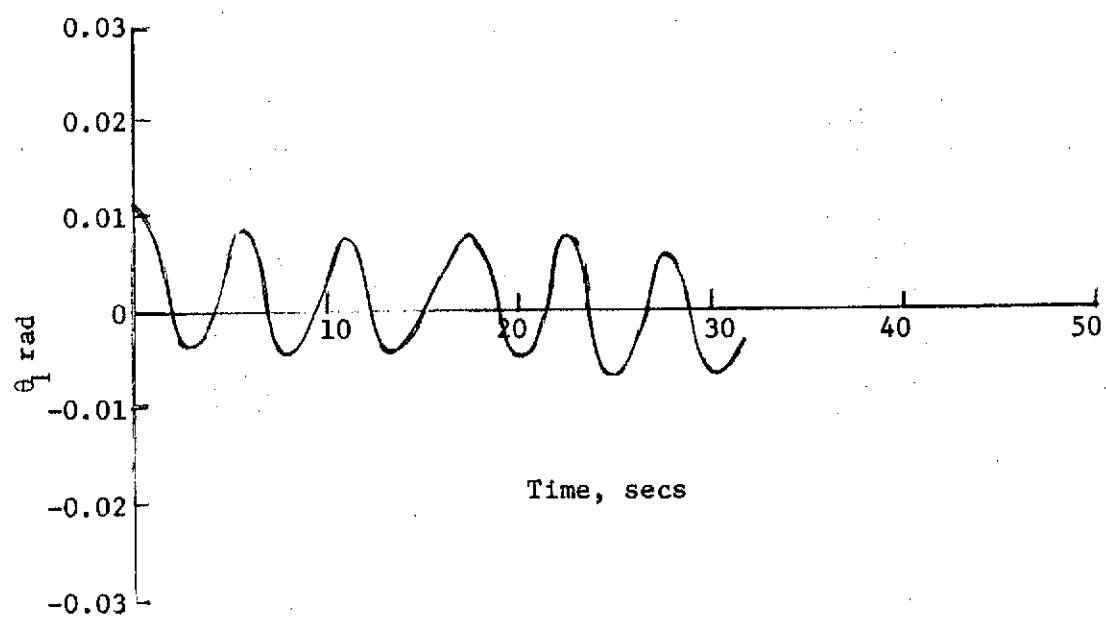


Figure 21. Motion of Symmetric Teleoperator After Satellite Capture, Case 1.

while the precession rate and the spin rate of the combined mass is constant, the magnitude of the coning angle θ_1 is oscillatory in nature. However, the maximum value of θ_1 is less than 0.09 radians (0.55°), and hence is within the capabilities of the Attitude Control System of the teleoperator Control Unit. Figure 22 shows the variation of the coning angle for the combined body, when the spin rate of the hand of the teleoperator differs from the spin rate of the satellite by 30%, while the precession rate and coning angle are exactly matched. It is seen that, again, the precession and spin rates for the combined body are constant and the coning angle undergoes irregular oscillations, though smaller in magnitude. Figure 23 shows the motion of the combined body when only the angle of the hand differs from the coning angle of the satellite by 5° . The oscillations in the magnitude of the coning angle θ_1 are fairly regular, and the value of the peak magnitude decreases slowly with time and is well within the ACS capabilities.

Figure 24 shows the motion of the combined body when the precession rate of the spindle differs from the precessional velocity of the satellite by 10%. Once again, the magnitude of the coning angle θ_1 for the combined body undergoes oscillations, with peaks slowly decreasing with time. The peak value is about 0.53° and well within the capacity of the ACS of the teleoperator Control Unit.

Figure 25 shows the motion of the combined mass when the angular rate of the spindle differs by 5%, the angle of hand by 5° , and the spin rate of the hand by 30% from the angle and angular rates of the satellite. It is seen that the oscillations in the coning angle θ_1 of

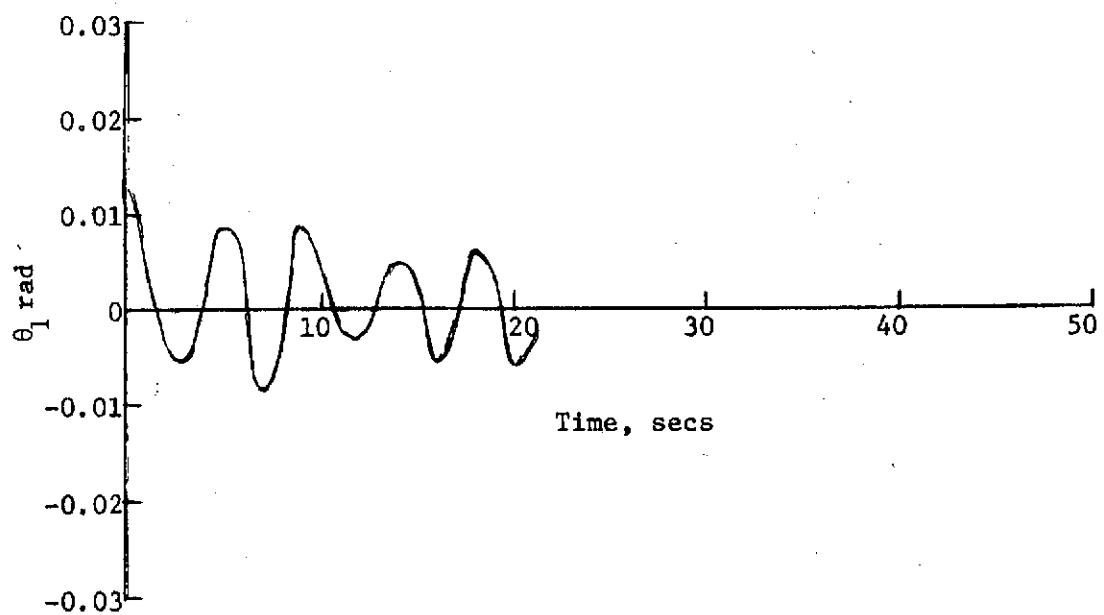


Figure 22. Motion of Symmetric Teleoperator After Satellite Capture, Case 2.

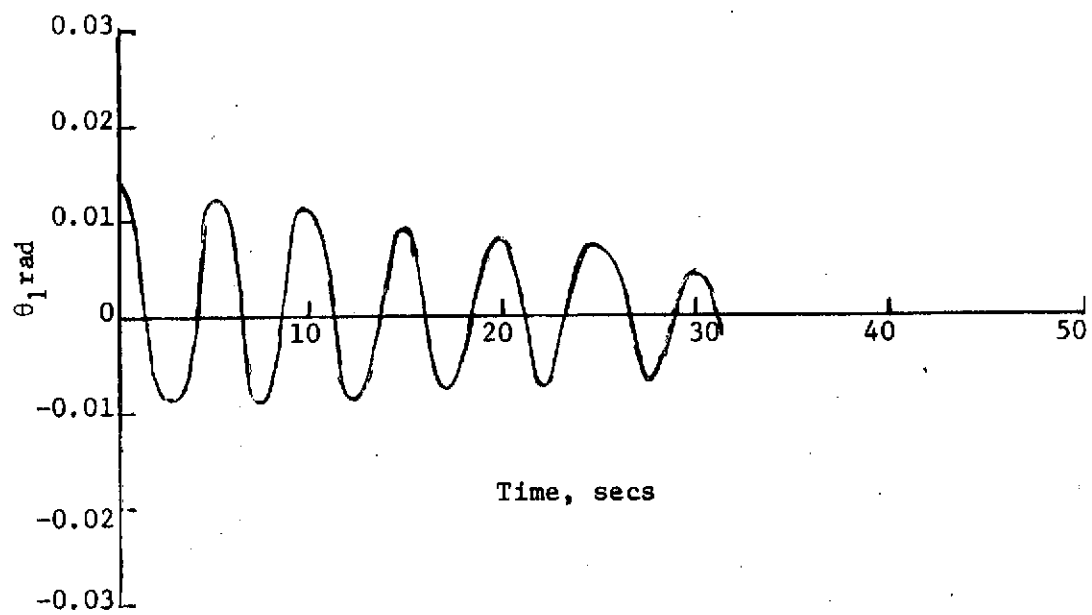


Figure 23. Motion of Symmetric Teleoperator After Satellite Capture, Case 3.

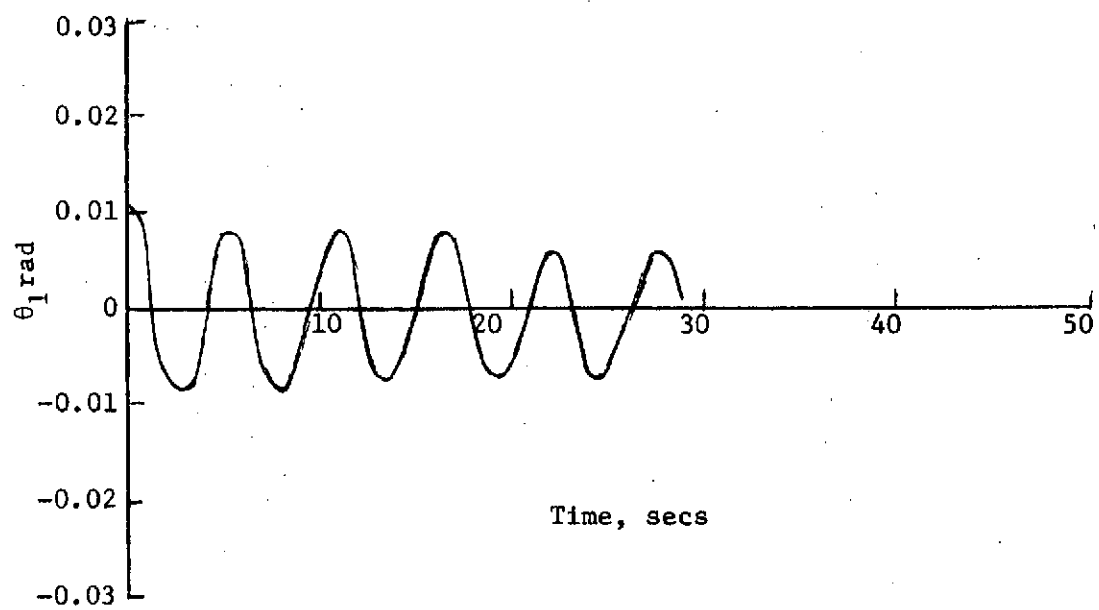


Figure 24. Motion of Symmetric Teleoperator After Satellite Capture, Case 4.

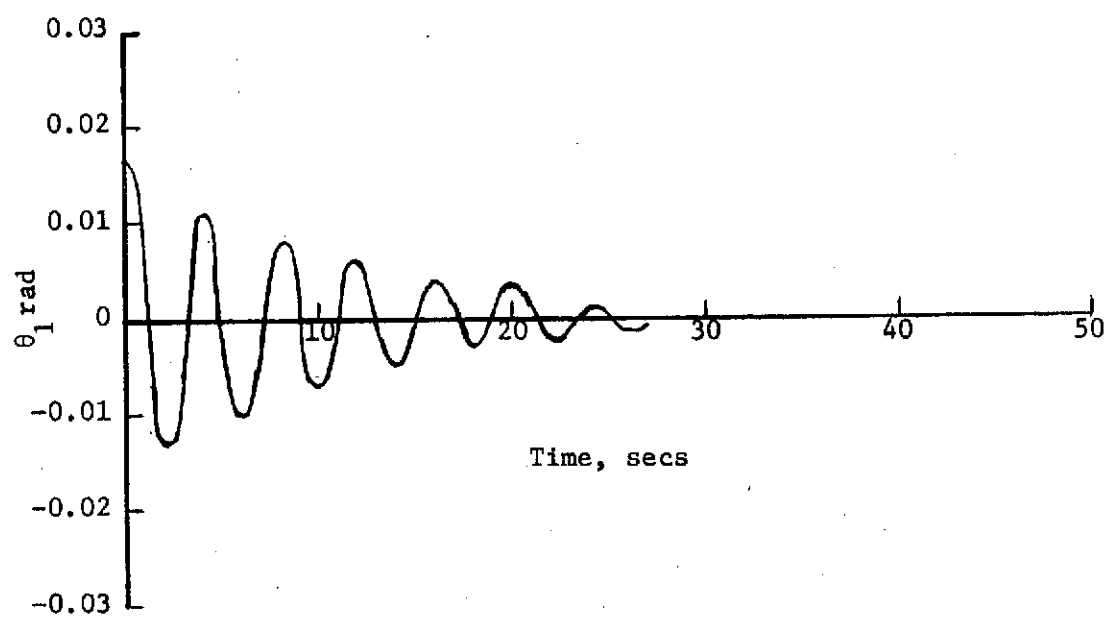


Figure 25. Motion of Symmetric Teleoperator After Satellite Capture, Case 5.

the combined body die out within 25-30 secs., while the angular rates remain constant. Figure 26 shows the motion when the spin velocity of the spindle differs by 10% from the precessional velocity of the satellite, the angle of the hand by 5° from the coning angle of the satellite, and the spin velocity of the hand by 30% from the spin velocity of the satellite. This is the worst case anticipated during the capture. The coning angle θ_1 is initially about 0.6° but again dies down within 25-30 secs.

Thus, it is found that with the modifications indicated in the design of the teleoperator, it will be able to capture the satellite successfully without itself going into an unstable spin-tumble mode. The maximum coning angles are well within the capability of the Attitude Control System of the teleoperator Control Unit.

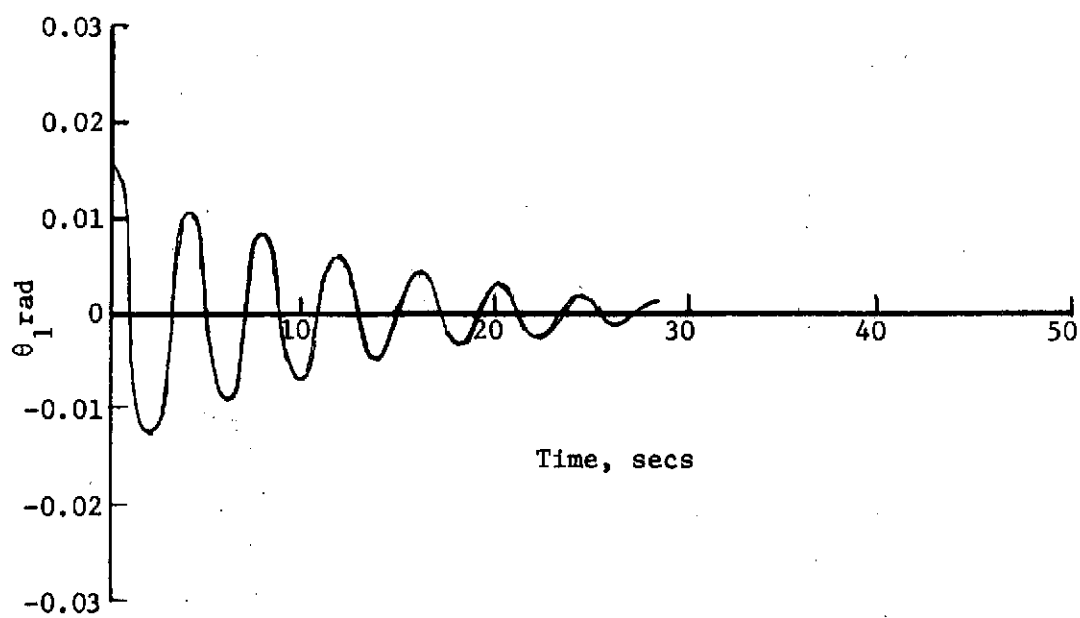


Figure 26. Motion of Symmetric Teleoperator After Satellite Capture, Case 6.

Chapter V

CONCLUSIONS

A detailed study was presented of the motion of a symmetric satellite under the influence of the passivating torques and of the motion of the combined teleoperator-satellite system, with misalignment in their angular momentum vectors. It was found that of the many torque functions that could be applied, a constant torque would passivate the motion in its direction of application faster than other forms of torque. For passivating the satellite motion simultaneously in all three directions, i.e. $\dot{\psi}$, $\dot{\theta}$, and $\dot{\phi}$, it was found that the best method would be to apply a constant torque on all the three axes, discontinue the despinning torque when the spin rate goes to zero, discontinue the detumbling torque when the precession is nullified, and finally decone with the deconing torque. The whole operation would take about 40 secs. It is concluded that no general procedure would suit all satellites. A particular procedure of passivating would have to be developed after observing the approximate spin and tumble rates of the particular satellite to be retrieved. It was also found that with modifications in the design of the teleoperator which is mentioned in the Appendix, it is possible to successfully capture the disabled satellite (before starting the passivation) without the teleoperator going into an unstable spin-tumble mode. The maximum coning angle after the capture of the satellite, even in the worst case, was of such magnitude to be well within the capability of the Attitude Control System of the teleoperator Control Unit.

REFERENCES

1. _____, "Teleoperator Technology and System Development," Final Technical Report Prepared under NASA Contract NAS 8-27021, Bell Aerospace Co., Report No. 8586-950001A, April 1972.
2. _____, "Preliminary System Design Criteria for Free-Flying Teleoperator Systems (FFTO) Satellite Retrieval Mission," Final Report Prepared under NASA Contract NAS 8-27021, Bell Aerospace Co., Report No. 8586-950003, June 1972.
3. Faile, G. C., Counter, D. N., and Bourgeois, E. J., "Dynamic Passivation of a Spinning and Tumbling Satellite Using Free Flying Teleoperator," Internal Report, NASA Marshall Space Flight Center, Huntsville, Alabama.
4. Martz, C. W., "Method for Approximating the Vacuum Motions of Spinning Symmetrical Bodies with Nonconstant Spin Rates," NASA TR R-115, 1961.
5. Greenwood, D. T., Principles of Dynamics, Prentice-Hall, Inc., New Jersey, 1965, Chapter 8.
6. Whittaker, E. T., A Treatise on the Analytical Dynamics of Particles and Rigid Bodies, Dover Publications, New York, Fourth Edition, 1944. pp. 144-151.
7. Thornton, W. G., Private Communication, NASA George C. Marshall Space Flight Center, Huntsville, Alabama, May 1973.

APPENDIX

TELEOPERATOR DESIGN MODIFICATIONS

The teleoperator and the satellite models used for analyzing the motion of the combined satellite-teleoperator system are discussed here. The weight and inertia properties of the satellite model used and of the teleoperator, as developed in present stages of design,⁽⁷⁾ are described in Figure 27. However, as is described in Chapter IV, this asymmetric teleoperator design appears unstable without complex attitude thrusting. As is obvious, there will be a certain interval of time from the instant when the teleoperator arm and hand are spun up to synchronize with the angular rates of the satellite, to the instant when it actually grasps the satellite. Hence, an improvement in this design of teleoperator is imperative, and this is illustrated in Figure 28. This symmetric teleoperator was found to be completely stable when its arm and hand were spun up. The additional inertia added to the case or the control unit of this teleoperator was necessary in view of the fact that, even though stable by itself, the teleoperator (without this additional inertia properties added to the case, in the xy plane) would quickly tumble over after holding the spinning and precessing satellite. This is because of the large asymmetry of the combined teleoperator-satellite system in the absence of indicated inertia properties. In all the discussions in Chapters III and IV, only this modified design of the teleoperator is considered for analyzing the motion of the combined teleoperator-satellite system.

ORIGINAL PAGE IS
OF POOR QUALITY

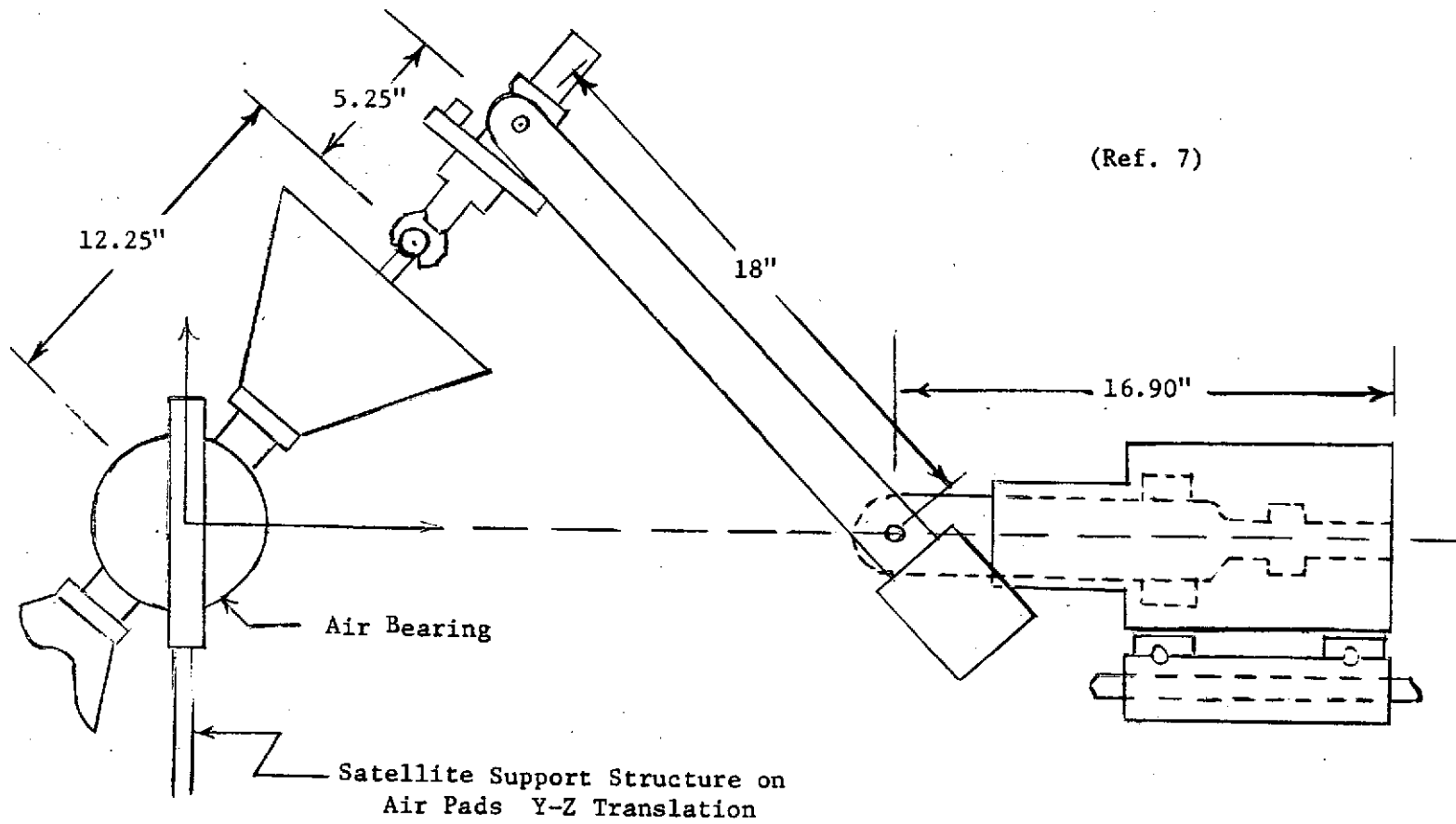
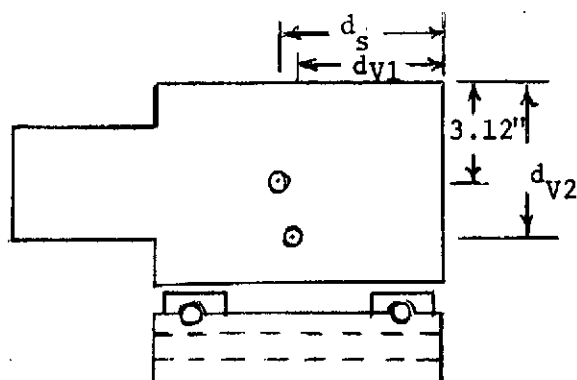


Figure 27. Weight and Inertia Properties of Satellite Despin Model and Teleoperator.



Case: Translates in
Y and Z Directions

Y Direction:

Weight = 18.056 lb.

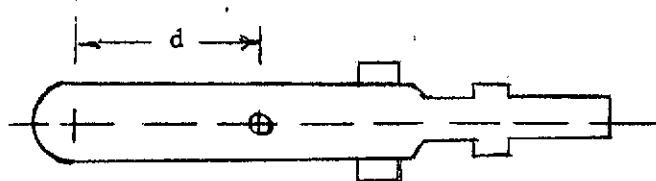
CG: $d_s = 4.983$ in.

Z Direction:

Weight = 30.491 lb.

CG: $d_{v1} = 4.644$ in.

$d_{v2} = 4.871$ in.

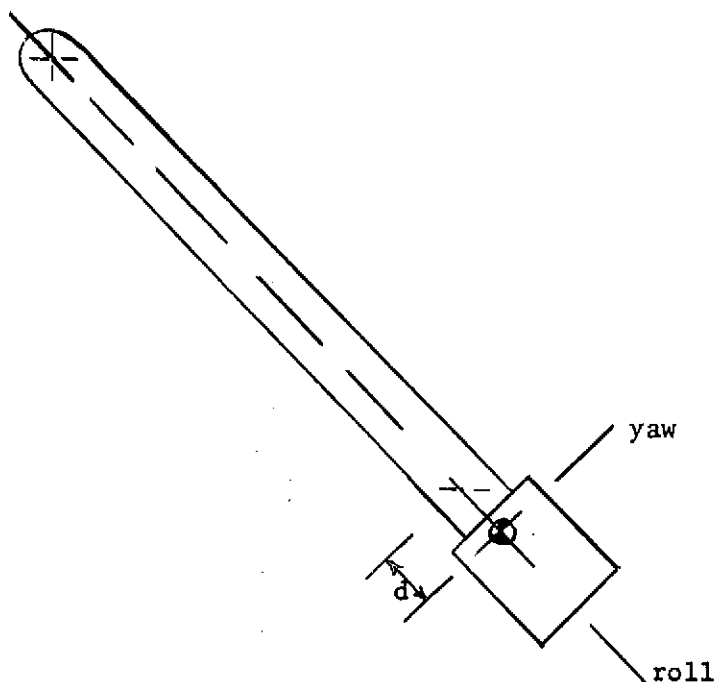


Spindle:

Weight = 7.066 lb.

$d = 5.57$ in.

$I_{roll} = 2.2496 \times 10^{-3} \text{ SL ft}^2$



Forearm:

Weight = 42.046 lb.

$d = 1.44$ in.

$I_{roll} = .14225 \text{ SL ft}^2$

$I_{pitch} = .159393 \text{ SL ft}^2$

$I_{yaw} = .291837 \text{ SL ft}^2$

ORIGINAL PAGE IS
OF POOR QUALITY

Figure 27. (continued)

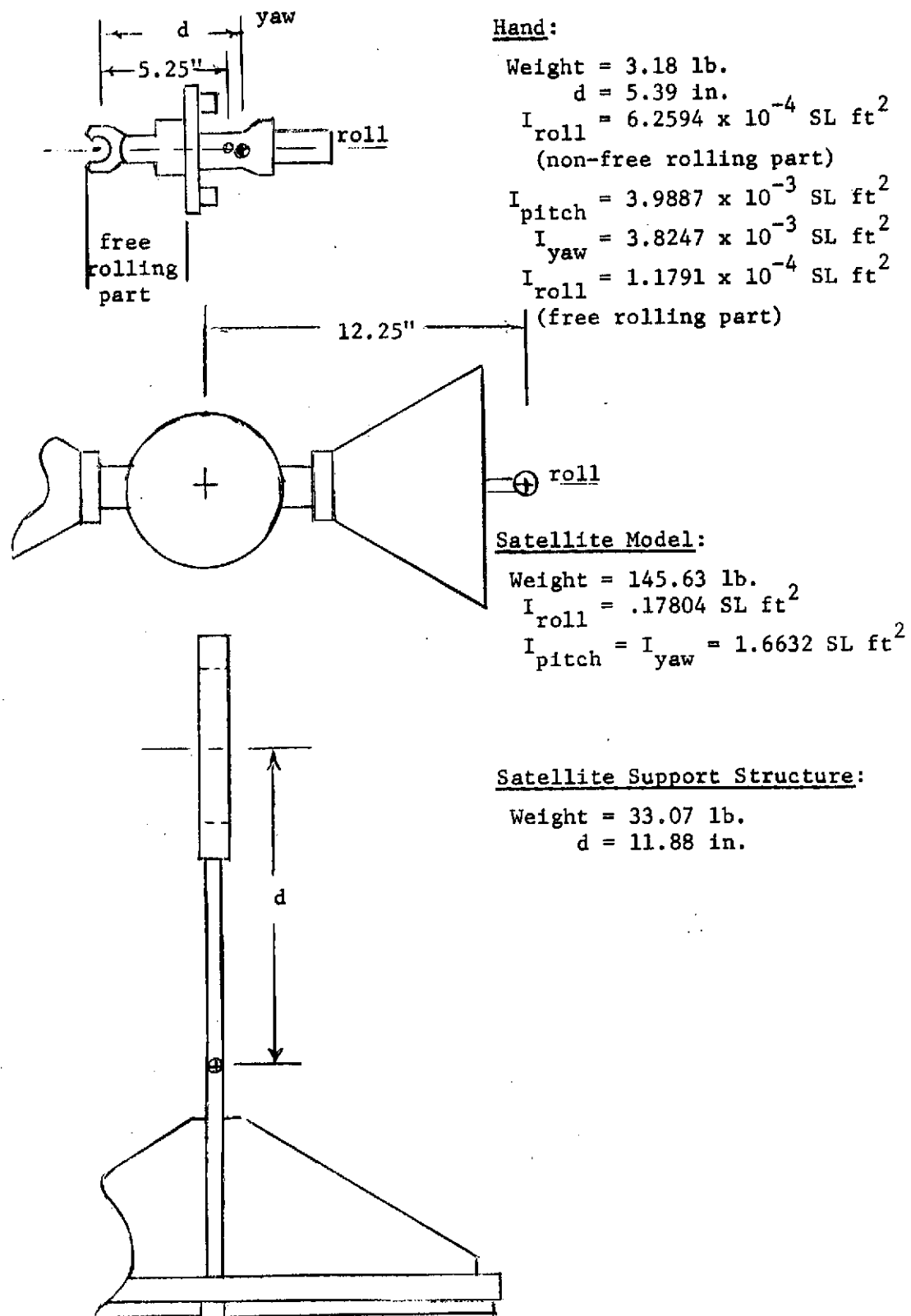


Figure 27. (continued)

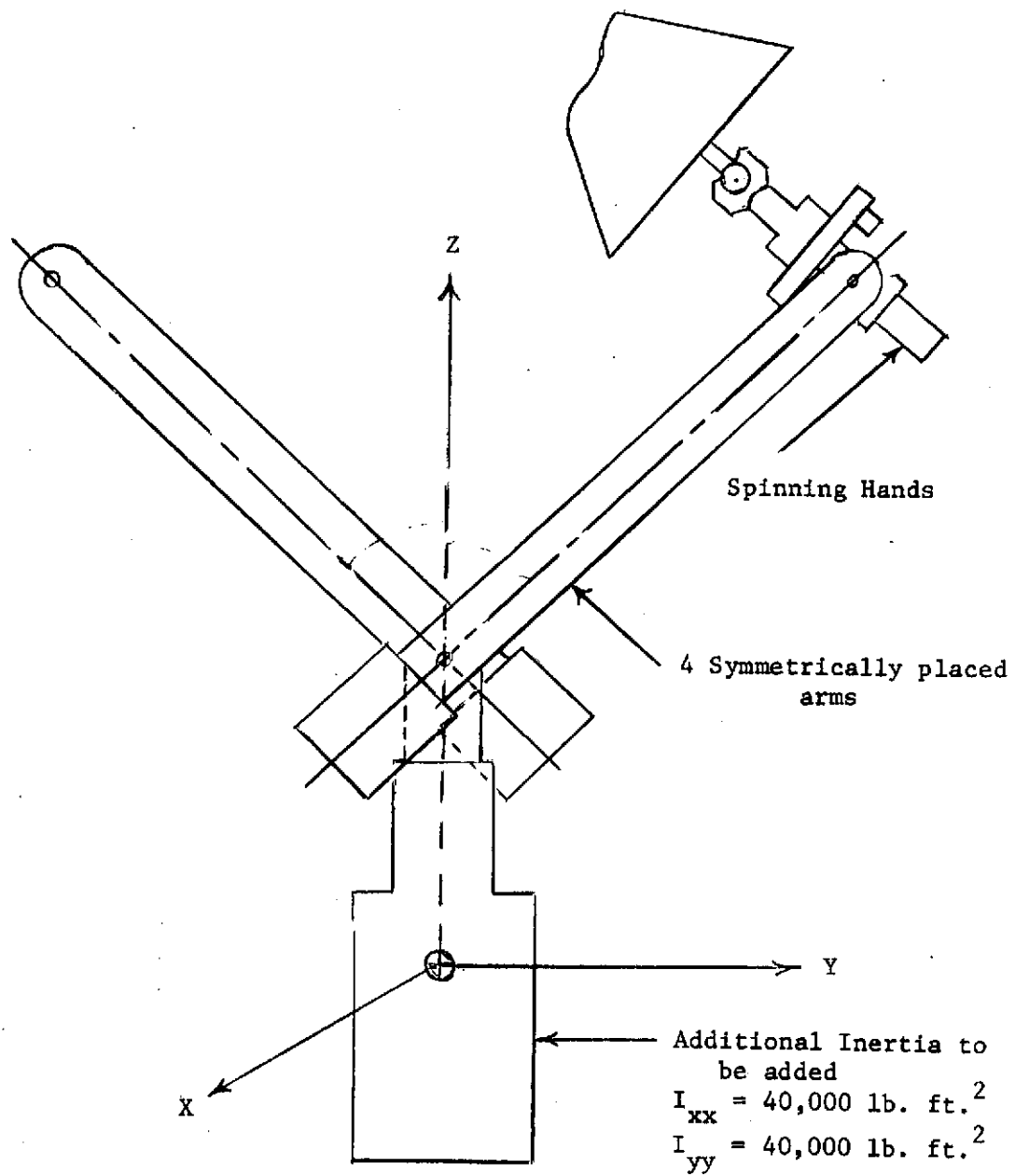


Figure 28. Modified Design of Teleoperator.